Weak interactions involving neutral currents

V. M. Shekhter

Leningrad Institute of Nuclear Physics, USSR Academy of Sciences
Usp. Fiz. Nauk **119**, 593–632 (August 1976)

This review is concerned with processes in which neutrinos are scattered (elastically or inelastically) by nucleons or electrons as a result of weak interactions involving neutral currents. The experimental data are summarized in detail and the restrictions which these data impose on the structure of the neutral currents are analyzed. Two particular gauge theories of the weak interaction are discussed, namely the well-known Weinberg-Salam model and the so-called vector model; both variants are in agreement with experiment for some appropriate value of the Weinberg angle or other analogous free parameter.

PACS numbers: 12.30.Cx, 13.15.+g

CONTENTS

1. INTRODUCTION

It has long been considered doubtful, or at any rate unproved, that there exists a weak interaction due to neutral currents. Experimental observations of neutral currents were made fairly recently, at the end of 1973. Their discovery led to a reappraisal of the generally accepted ideas about the nature of the weak interaction. In particular, it was found that the weak interaction is not universal: its coupling constants are different for different particles. On the other hand, hopes arose of constructing a future realistic renormalizable theory incorporating not only the weak interaction, but also the electromagnetic and possibly the strong interaction. It is not obvious how to construct such a theory without neutral currents. The new scheme would probably be "universal" in some different and "deeper" sense.

The existence of neutral currents is also important for an understanding of astrophysical phenomena. It is well known that the processes which take place in stars involve the transfer of large amounts of energy to neutrinos or antineutrinos, which then propagate into interstellar space. The presence of neutral currents should show up in the energy balance. In studying certain particular problems, such as supernova explosions, it is also important to consider the effects of coherent interactions of neutrinos with heavy nuclei as a whole as a result of neutral currents.

The study of weak interactions involving neutral currents is only just beginning. The data of most experiments should be regarded as preliminary. Nevertheless, certain conclusions can already be drawn about the nature of these interactions. The purpose of the present review is to give a systematic exposition of the experimental results obtained up to the middle of 1975 and their theoretical consequences. The discussion is limited to processes involving neutrinos, which are certainly governed by the weak interaction. Proposals are also made for many experiments which could in principle reveal effects of parity nonconservation due to the weak interactions involving neutral currents in the background of electromagnetic transitions in atomic physics, but all these experiments are very difficult and have so far not been carried out. A detailed discussion of these problems can be found in the reviews[1].

2. THEORY AND EXPERIMENT

A. Prehistory

What is now the "canonical" scheme of weak-interaction theory was formulated in 1958 by Feynman and Gell-Mann[2] and Marshak and Sudarshan.[3] The only significant extension of this scheme, due to Cabibbo,[4] was its generalization to processes involving strange particles.

The scheme is based on a current J_α, which consists of three components, namely an electron, muon, and hadronic component:

$$J_\alpha = (\bar{\nu}_e O_\alpha e) + (\bar{\nu}_\mu O_\alpha \mu) + (\bar{u} O_\alpha d_C), \qquad O_\alpha = \gamma_\alpha (1+\gamma_5). \tag{1}$$

The last term in J_α is expressed in terms of quark operators, for which we adopt the Feynman notation u, d, s, and

$$d_C = d\cos\theta_C + s\sin\theta_C, \tag{2}$$

TABLE I. Upper limits on hadron decays into a neutral lepton pair.

Decay	Relative decay probability with respect to the full width	Decay	Relative decay probability with respect to the full width
$K_L^0 \to \mu^+ + \mu^-$	$(1.0^{+0.7}_{-0.4}) \cdot 10^{-8}$	$K^\pm \to \pi^\pm + \mu^+ + \mu^-$	$< 2.4 \cdot 10^{-6}$
$\to e^+ + e^-$	$< 1.6 \cdot 10^{-9}$	$\to \pi^\pm + e^+ + e^-$	$(2.6 \pm 0.5) \cdot 10^{-7}$
$\to e^\pm + \mu^\mp$	$1.6 \cdot 10^{-9}$	$\to \pi^\pm + \bar{\nu} + \nu$	$< 5.6 \cdot 10^{-7}$
$K_S^0 \to \mu^+ + \mu^-$	$< 3 \cdot 10^{-7}$	$\to \pi^\pm + (e^\pm + \mu^\mp)$	$< 1.4 \cdot 10^{-8}$
$\to e^+ + e^-$	$< 3.5 \cdot 10^{-4}$	$\to \mu^\pm + \nu + \bar{\nu} + \nu$	$< 6 \cdot 10^{-6}$
		$\Sigma^+ \to p + e^+ + e^-$	$< 7 \cdot 10^{-6}$

where θ_C is the Cabibbo angle. Experimentally,[5]

$$\sin \theta_C = 0.230 \pm 0.003. \tag{3}$$

The small value of the angle θ_C is related to the suppression of the β-decay coupling constant of hyperons in comparison with the coupling constant for neutron decay. The current is "charged," since, when acting on any state, it alters its charge.

The weak-interaction Hamiltonian in the scheme of Feynman and Gell-Mann is quadratic in the current J_α:

$$\mathcal{H}_W = \frac{G}{\sqrt{2}} J_\alpha J_\alpha^+; \tag{4}$$

here G is a constant with dimensions (mass)$^{-2}$. To a good approximation,

$$G = 10^{-5} m_N^{-2}. \tag{5}$$

The weak interaction in the form (1)–(4) is in good agreement with a large quantity of data on the weak decays of hadrons and muons, as well as the recently measured cross sections for νN and $\bar{\nu} N$ interactions. A characteristic feature of this interaction is that it contains only charged currents.

The main experimental argument against the presence of neutral, i.e., charge-conserving, currents in $\mathcal{H}_W$ was the absence of kaon decays into neutral lepton pairs. The upper limits on the probabilities of such decays are given in Table I. (These results are taken mainly from the tables of[6], where references to the original papers can also be found.) A distinguishing feature of all the reactions listed in Table I is the occurrence of a strangeness-changing hadronic transition. The absence of such transitions is by no means a proof that reactions involving a neutral lepton pair cannot occur when the strangeness of the hadrons is unchanged. The question of whether such reactions do occur remained unresolved until 1973.

As regards purely leptonic experiments, prior to 1973 it was known only that the decays $\mu^\pm \to e^\pm e^+ e^-$, $\mu^\pm \to e^\pm \gamma$, and $\mu^\pm \to e^\pm \gamma\gamma$ do not occur (Table II). Of course, this indicates not the absence of neutral currents, but conservation of the muon number (which is equal to 1 for μ^- and ν_μ, -1 for μ^+ and $\bar{\nu}_\mu$, and 0 for the other particles). The possible existence of currents such as $(\bar{\nu}_\mu \nu_\mu)$ or $(\bar{e}e)$ and scattering of the muonic neutrino by the electron, for example, also remained an open question.

It appears that Bludman[7] was the first to suggest that there might exist neutral diagonal currents such as $(\bar{e}e)$, $(\bar{\nu}\nu)$, or $(\bar{p}p)$. Possible processes due to such currents were actively discussed in the late 50's and early 60's, particularly by Soviet physicists. Various estimates were made of the cross sections for elastic scattering of the muonic neutrino by the electron and proton, the possible excitation of nuclei by the neutral current, the interference between the contributions of the charged and neutral currents in the interaction of the electronic neutrino with the electron, and other effects.[8–12] All such experiments are very complex, and they became feasible only ten years later.

Until the early 70's, there existed only a single and indeed rather ambiguous piece of evidence for neutral currents, namely the $\Delta I = 1/2$ rule for non-leptonic decays of kaons and hyperons. The term in the Hamiltonian (1) which is responsible for such decays has the form

$$\frac{G}{\sqrt{2}} \cos\theta_C \sin\theta_C (\bar{u} O_\alpha s)(\bar{d} O_\alpha u) + \text{H.c.} = \frac{G}{\sqrt{2}} \cos\theta_C \sin\theta_C (\bar{u} O_\alpha u)(\bar{d} O_\alpha s) + \text{H. c.} \tag{6}$$

where the equality is due to the antisymmetry of the $V-A$ variant of the four-fermion interaction with respect to the Fierz transformation of the operators.

The expression (6) contains a product of currents with $I = 1$ and $I = 1/2$ and therefore leads to transitions with both $\Delta I = 1/2$ and $\Delta I = 3/2$. To eliminate the possibility of the latter, we must add to (6) the term

$$\frac{G}{\sqrt{2}} \cos\theta_C \sin\theta_C (\bar{d} O_\alpha d)(\bar{d} O_\alpha s) + \text{H. c.} \tag{7}$$

after which the sum contains the expression $(\bar{u} O_\alpha u) + (\bar{d} O_\alpha d)$ with $I = 0$ and the current with $I = 1$ drops out. Thus, after multiplication by $(\bar{d} O_\alpha s)$, the $\Delta I = 1/2$ rule is satisfied.

On the other hand, the expression (7) has the form of a product of neutral currents, one of which, $(\bar{d} O_\alpha s)$, in conjunction with the analogous leptonic expressions, would lead to precisely the decays listed in Table I, which do not occur experimentally. Consequently, even if the current $(\bar{d} O_\alpha s)$ does exist, it cannot be associated with the leptons. It has so far not been possible to construct a reasonably elegant scheme which incorporates the interaction (7) but excludes the semileptonic strangeness-changing decays (see Table I). For this reason, many authors prefer not to introduce

TABLE. II. Upper limits on the non-neutrino decays of muons.

Decay	Relative decay probability with respect to the full width
$\mu^\pm \to e^\pm + e^+ + e^-$	$< 6 \cdot 10^{-9}$
$\to e^\pm + \gamma$	$< 2.2 \cdot 10^{-8}$
$\to e^\pm + \gamma + \gamma$	$< 1.6 \cdot 10^{-5}$

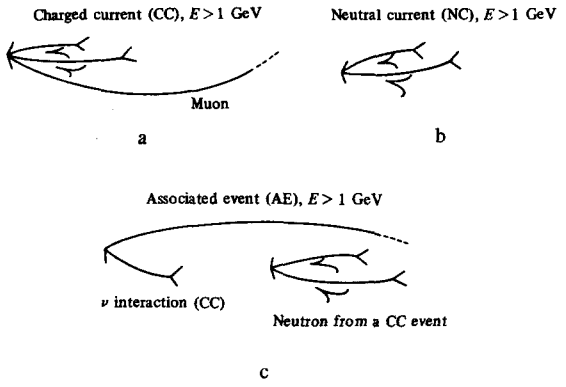

FIG. 1. Classification of events in the experiment carried out in the heavy-liquid chamber "Gargamelle."

the current ($\bar{d}O_\alpha s$) at all in the theory and to attribute the $\Delta I=1/2$ rule to some dynamical "enhancement."

To summarize, we can say that for a period of almost 15 years the theory of weak interactions contained no neutral currents and that most physicists have seen no need to introduce them.

B. Gauge theories

The theoretical situation changed in 1971, when t'Hooft[13] demonstrated the existence of a new class of renormalizable theories in which the interaction is mediated by vector gauge fields; these fields must necessarily include both charged and neutral components. The theory of this type which was of the greatest interest is the Weinberg-Salam model,[14,15] which had been proposed four years earlier and which provides a rather elegant unification of the weak and electromagnetic interactions. (The properties of such theories are discussed, for example, in the review[16].)

The possibility of rendering weak-interaction theory renormalizable is very attractive; it is for this reason that the Weinberg-Salam model, which remained in the background for nearly five years, suddenly became the center of attention. (Various other models had also been proposed, but they generally include a large number of hitherto unobserved particles.) Since this model involves neutral currents, the question of whether such currents exist in the weak interaction was once again raised. It had somehow become almost obvious that there are no neutral currents. A series of new experiments were carried out.

C. Processes involving charged and neutral currents

Neutral currents cannot lead to any observable consequences in the decays of non-strange particles. Their effects must therefore be sought in some other processes. The simplest possibility is to look for such currents in reactions due to neutrino-hadron or neutrino-electron interactions. The fact that the neutrino has no interactions apart from the weak interaction (as is usually the case for elementary particles, gravitation is unimportant) allows a strong suppression of the possible background. Since the cross sections for the weak interactions of neutrinos with electrons or nucleons rise with energy, it is advantageous to work with neutrino beams in large accelerators.

Figure 1 shows the method of distinguishing experimentally between neutrino-nucleon interaction processes involving charged currents (CCs) and those involving neutral currents (NCs), i.e.,

$$\nu_\mu(\bar{\nu}_\mu)+N\to\mu^-(\mu^+)+\text{hadrons (CC)} \tag{8}$$

$$\nu_\mu(\bar{\nu}_\mu)+N\to\nu_\mu(\bar{\nu}_\mu)+\text{hadrons (NC)} \tag{9}$$

The final state in the reaction (8) contains both hadrons and a muon; in the reaction (9) it contains only hadrons, for the neutrino is not observed. Thus the appropriate criterion for an event due to NCs is the absence of a muon. Such events can be recognized by virtue of the characteristic property of the muon which makes it possible to distinguish its tracks from those of hadrons, namely a relatively large path length with no interactions.

As to neutrino-electron scattering,

$$\nu_\mu(\bar{\nu}_\mu)+e^-\to\nu_\mu(\bar{\nu}_\mu)+e^-, \tag{10}$$

this process is characterized by the appearance of only a single track—that of the recoil electron.

In all cases, it is of course necessary to take into account the possible presence of a background of neutral particles (such as neutrons, K_L^0 mesons, or photons) and the fact that the muon in an event of type (8) might somehow escape detection. These circumstances are the principal difficulties in the experimental investigation of neutral currents.

D. Neutrino experiments

Weak-interaction processes involving NCs and CCs are generally studied using the same experimental apparatus. The traditional experimental scheme is shown in Fig. 2. A proton beam extracted from an accelerator is incident on a target, in which charged pions and kaons are produced. These particles then pass through focusing magnets (a "horn"), which make the beam narrower and separate the mesons having a charge of one particular sign (in the case of the "narrow" beams at Batavia, particles having a definite momentum are also selected). Next, the pions and kaons move through a tunnel, which is sufficiently long for them to decay into muons and neutrinos. At the end of the tunnel there is a shield, which absorbs all particles except

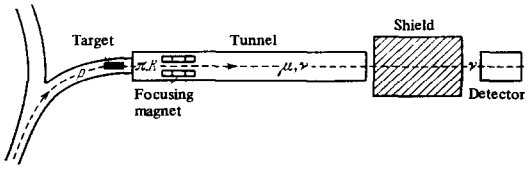

FIG. 2. Scheme of the neutrino experiments using accelerators.

TABLE III. Neutrino experiments using accelerators.

Laboratory	Argonne	CERN	Brookhaven	Serpukhov	Batavia*
Proton energy, GeV	12	26	29	69	300–400
Target	Beryllium 0.6 m	Beryllium 1.3 m	Sapphire	Sapphire, copper, aluminum	Iron, 0.3 m
Tunnel length, m	27	70	45	140	350
Shield	Iron, 13 m	Iron, 22 m	Iron, 30 m	Iron, 70 m	Earth a) 1000 m b) 500 m
Neutrino energy, GeV	0–3	1–10	1–10	2–20	a) 5–200 b) 20–150
Maximum of the spectrum, GeV	0.5	2	2	4	a) 20 or 50 and 160 b) 45 and 125
Detectors	12-ft bubble chamber	1) 8-m freon chamber "Gargamelle" 2) 1.2-m propane chamber 3) Aluminum spark chambers (20 m)	1) 7-ft bubble chamber 2) Aluminum spark chambers	1) Steel target, spark chambers 2) Heavy-liquid chamber SKAT	a) Liquid scintillator, spark chambers b) Steel target, spark chambers c) 15-ft bubble chamber

*The variants a) and b) correspond to the experiments of the Harvard-Pennsylvania-Wisconsin and Caltech-Fermilab groups, respectively. The 15-ft bubble chamber operates with a wide beam a).

neutrinos. A neutrino detector is placed behind the shield.

The parameters of various neutrino experiments are listed in Table III, from which it can be seen that neutrino beams are available at only five of the largest laboratories of the world at the present time. The neutrino spectra are given in the Appendix. The characteristics of the detectors, i.e., the apparatus for recording neutrino interactions, are given later in connection with particular experiments.

The currently available experimental data can be divided into three categories.

1) Inclusive experiments, in which a summation is made over all hadronic states in the reaction (9). There are three experiments of this type: the CERN "Gargamelle" Neutrino Collaboration, the Harvard-Pennsylvania-Wisconsin Collaboration, and the Caltech-Fermilab Collaboration.

2) Exclusive processes, in which completely well-defined hadrons are detected. The following processes have been studied:

$$\left.\begin{array}{ll} \nu_\mu + p \to \nu_\mu + p & \text{(CERN, Argonne),} \\ \nu_\mu + N \to \nu_\mu + N' + \pi & \text{(Argonne, Columbia-Brookhaven, CERN),} \\ \nu_\mu + N \to \nu_\mu + N + \pi^+ + \pi^- & \text{(Brookhaven),} \\ \nu_\mu + p \to \nu_\mu + p + 2\pi^+ + 2\pi^- & \text{(Brookhaven),} \\ \nu_\mu + N \to \nu_\mu + \Lambda + K & \text{(Argonne, CERN),} \\ \bar{\nu}_e + d \to \bar{\nu}_e + p + n & \text{(Irvine-Savannah River reactor).} \end{array}\right\} \quad (11)$$

3) Scattering of muonic neutrinos and antineutrinos by electrons, i.e., the reaction (10). This experiment has been carried out at CERN. Scattering of electronic antineutrinos by electrons has been studied using the Savannah River reactor.

All three types of processes are considered in turn in Secs. 3–5.

3. INCLUSIVE EXPERIMENTS

A. The CERN experiment[17,18]

This experiment was carried out in the "Gargamelle" bubble chamber of length 5 m and diameter 1.8 m, filled with freon CF_3Br. The operative volume of the chamber was 8 m^3, and the experiment utilized an effective volume of 3 m^3. The neutrino energy was distributed over a spectrum ranging from 1 to 10 GeV, with a maximum near 2 GeV (see Table III and the Appendix).

The events in the chamber were divided into three categories, designated CC (charged currents), NC (neutral currents), and AE (associated events). In the CC events (see Fig. 1a), one track is muon-like (a large path length and no interactions with nuclei), while the others correspond to hadrons. In the NC events (Fig. 1b), all the particles are definitely hadrons. The AE events (Fig. 1c) are CC events which involve a second purely hadronic NC-type star, which obviously originates from a neutron-nucleus interaction (the track of the neutron is not observed), the neutron having been

TABLE IV. The inclusive experiment in the "Gargamelle" bubble chamber (CERN, 1 film = 750 photographs): the numbers of events.

	1973		1974	
	ν	$\bar{\nu}$	ν	$\bar{\nu}$
CC/film	413/?	113 ?	218/66 = 3.20±0.45	
NC/film	102/111 = 0.92±0.13	63/278	189/209 = 0.90±0.10	70/298
AE/film	15/111 = 0.13±0.04	= 0.23±0.01	42/268 = 0.15±0.02	= 0.23±0.01
R	0.23±0.03	12/276	0.217±0.026	14/328
$\left(\frac{\sigma_{\bar{\nu}}}{\sigma_{\nu}}\right)_{NC}$		= 0.04±0.01		= 0.04±0.01
		0.46±0.09		0.43±0.12
	0.78±0.18		0.74±0.23	

produced in the primary neutrino collision. Those events in which the observed energy of the hadrons exceeded 1 GeV were selected. The results are shown in Table IV, which gives both the number of events of each type and the number of photographs which were analyzed.

The background was due primarily to neutrons produced by neutrino interactions in the magnet and shield. A Monte-Carlo calculation showed that the number of such events should be 0.8±0.4 of the number of AE-type events, in which both interactions are seen. Thus the total neutron background was about 10%.[19]

The authors gave two further arguments that the NC events were due to incident neutrinos or antineutrinos. First, both the CC and NC events were uniformly distributed over the length of the chamber along the direction of the neutrino beam. At the same time, the number of neutron stars induced by a proton beam in a special experiment decreased along the axis of the chamber, since the neutron interaction length (~ 70 cm) is small in comparison with the dimensions of the operative region. Second, the ratio of the numbers of neutral and charged pions was roughly the same for the 42 AE-type events and 73 proton-induced neutron events (NEs) but was significantly different for the NC events (Table V). The probability that these ratios are equal (according to the χ^2 criterion) is ~ 10^{-4}. Thus we can regard these results as a demonstration that there exist non-muonic events induced by neutrinos or antineutrinos and hence events due to neutral currents.

It is customary to characterize the NCs by the ratio of the corresponding NC and CC cross sections, namely

$$R_{\nu}=\frac{\sigma(\nu_{\mu}+N\to\nu_{\mu}+\text{hadrons})}{\sigma(\nu_{\mu}+N\to\mu^{-}+\text{hadrons})},$$
$$R_{\bar{\nu}}=\frac{\sigma(\bar{\nu}_{\mu}+N\to\bar{\nu}_{\mu}+\text{hadrons})}{\sigma(\bar{\nu}_{\mu}+N\to\mu^{+}+\text{hadrons})}. \qquad (12)$$

It can be seen from Table IV that the same values of

TABLE V. The ratio $\pi^0/(\pi^+ + \pi^-)$ for the various types of events in the CERN experiment.

Observed hadron energy, GeV	AE	NE	NC
1—2	0.24±0.08	0.38±0.12	0.75±0.09
2—3	0.10±0.07	0.23±0.09	0.53±0.11
3—5	0.20±0.20	0.31±0.10	0.37±0.28
5—7	—	0.31±0.16	0.48±0.16

TABLE VI. The numbers of events in the HPW inclusive experiment (1973, $\nu:\bar{\nu}=3:1$).

CC	NC	Background	R
93	76	36	0.28±0.10

R_{ν} were obtained in 1973 and 1974, although the statistics of the ν_{μ} events were practically doubled. However, the situation was different in the case of $R_{\bar{\nu}}$. After a tripling of the statistics of the $\bar{\nu}_{\mu}$ events in 1975, there was a significant increase in the value of $R_{\bar{\nu}}$[20]:

$$R_{\bar{\nu}}=0.55+0.07,$$
$$\left(\frac{\sigma_{\bar{\nu}}}{\sigma_{\nu}}\right)_{NC}=0.96\pm0.18. \qquad (13)$$

The values of $R_{\bar{\nu}}$ in Table IV and in (13) include a correction for the admixture of neutrinos ν_{μ} in the antineutrino beam. In converting the values of $R_{\bar{\nu}}$ and R_{ν} into a ratio of antineutrino and neutrino cross sections involving neutral currents, allowance must be made for the fact that the corresponding cross sections involving charged currents are in the ratio 1 : 3. We shall return to this point later in Sec. 2D.

B. The HPW experiment[21-24]

The experimental arrangement of the Harvard-Pennsylvania-Wisconsin (HPW) group is shown in Fig. 3. It includes 70 tons of liquid scintillator (a calorimeter for measuring the total energy of the hadrons), spark chambers for detecting particle tracks, and a muon detector consisting of four iron toroids of thickness 1.2 m, separated by spark chambers.

As in the CERN experiment, the events in which no muons were detected were NC candidates, however, the calculated efficiency of muon detection in the original experiment[21] was 71%, so that the muons were not identified in a large fraction of the CC events (Table VI). If the detection efficiency were reduced to 0.55, all the NC events would be incorrectly identified CC events.

In the 1974 experiment,[22,23] the efficiency of muon detection was somewhat higher and the statistics were much better. Moreover, experiments were carried out using beams with different proportions of neutrinos and antineutrinos. This made it possible to determine

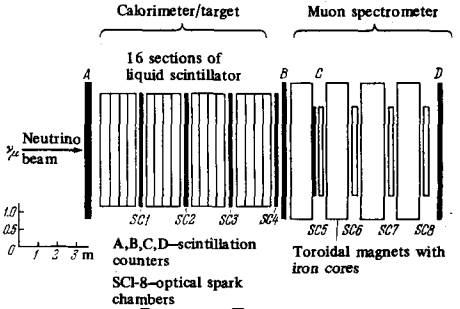

FIG. 3. Experimental scheme of the Harvard-Pennsylvania-Wisconsin (HPW) group at Batavia.

TABLE VII. The HPW inclusive experiment (1974).

Beam	Number of NC events	β	R
Broad (no focusing)	255	0.74±0.06	0.18±0.05
Broad (focused)	283	0.45±0.06	0.22±0.05
Narrow	100	0.12±0.05	0.34±0.12
»	188	0.98±0.01	0.13±0.06

$R_\nu = 0.12 \pm 0.04$, $R_{\bar\nu} = 0.32 \pm 0.08$, $\left(\frac{\sigma_{\bar\nu}}{\sigma_\nu}\right)_{NC} = 1.09 \pm 0.55$.

R_ν and $R_{\bar\nu}$ individually. The results are shown in Table VII, where the coefficient β characterizes the composition of the beam:

$$\beta = \frac{\nu_\mu}{\nu_\mu + \bar\nu_\mu} \tag{14}$$

and is determined from the cross sections for μ^- and μ^+ production due to the charged currents. Obviously,

$$R = R_\nu \beta + R_{\bar\nu}(1-\beta). \tag{15}$$

An attempt was also made in 1975 to obtain information about the correct variant of the weak interaction in the neutral current. This was done by constructing the dependence of R on the energy of the hadrons. This dependence is shown in Fig. 4 for two values of the ratio β. The calculated results for the $V-A$, $V+A$, V, and A variants are also shown in this figure. In spite of large experimental errors, the authors find that there are large numbers of high-energy hadrons even for the $V-A$ variant (more so than for the V, A, or $V+A$ variants). Even the possible existence of heavy leptons is not excluded.[24]

C. The Caltech-Fermilab experiment[25,26]

This experiment was carried out using narrow ν_μ and $\bar\nu_\mu$ beams of energy 45 and 125 GeV. The experimental arrangement, shown in Fig. 5, consisted of a 143-ton iron calorimeter (constructed of blocks of thickness 10 cm) and a toroidal magnet for muon identification.

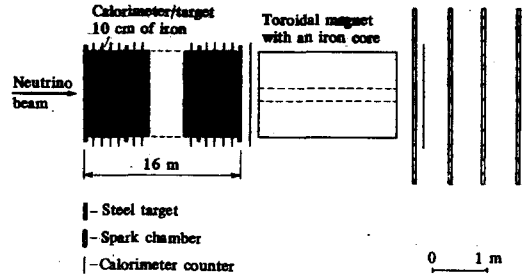

FIG. 5. Scheme of the Caltech-Fermilab experiment at Batavia.

The experimental analysis was based on the fact that the absorption in iron is different for hadrons ($\lambda_{abs} \approx 1$ m at $E = 100$ GeV) and for muons ($\lambda_{abs} \approx 1\ \text{m} \times E\ (\text{GeV})$). A study was made of those events involving an energy release in the calorimeter of at least 6 GeV. The particle having the greatest track length was selected in each such event, and the distribution of these particles with respect to the track length L along the direction of the neutrino momentum was constructed. This distribution is shown in Fig. 6 (ν_μ beam) and Fig. 7 ($\bar\nu_\mu$ beam). It is in good agreement with the calculated muon track length for $L > 1.5$ m, but it is found that the experimental values are much larger than the calculated values in the region $L \sim 1$ m, presumably as a result of purely hadronic events, which were of course attributed to NC interactions. The correctness of this assumption is confirmed by the fact that those events in the region of the peak near 1 m are uniformly distributed along the calorimeter. The hypothesis that these are "anomalous" CC events in which the energy of the muon is for some reason smaller than the energy of at least one of the hadrons is unacceptable, since the energy distribution of the hadrons for the events in the peak is not displaced towards larger energies in relation to the distribution for the "ordinary" CC events.

The results of the experiment are shown in Table VIII. The CC events were normalized to the region of

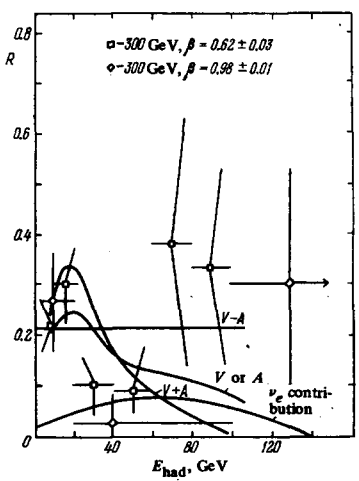

FIG. 4. The ratio of neutral to charged currents as a function of the hadron energy in the HPW experiment.

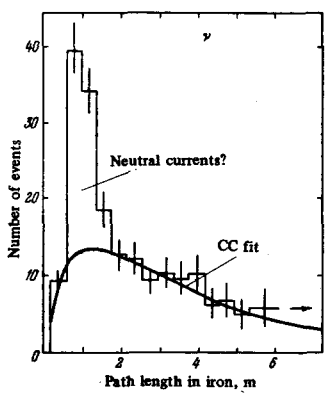

FIG. 6. Distribution with respect to the path length of the most energetic particle produced in the neutrino beam.

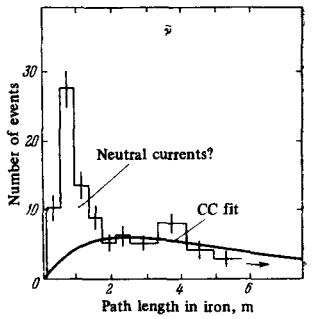

FIG. 7. Distribution with respect to the path length of the most energetic particle produced in the neutrino beam.

large path lengths ($L > 1.4$ m) in Figs. 6 and 7. It can be checked that this normalization is correct by considering a restricted range of L, such as 1.4 m $\leq L \leq 6.0$ m. The excess of the number of experimental events in the region $L < 1.4$ m over the number calculated assuming CCs was attributed to NCs.

The authors consider that their experimental values of R_ν and $R_{\bar{\nu}}$ given in Table VIII are preliminary and require further analysis. For example, an appreciable fraction of the events may be due to CC processes which occur when ν_μ and $\bar{\nu}_\mu$ of comparatively low energy (from the broad left-hand tail of the neutrino spectrum) collide with nucleons. In addition, the restriction $E_{had} > 6$ GeV is important. The extrapolation into the region of small E_{had} has a large uncertainty and depends in particular on the variant of the weak interaction. The possible deviation from this result is shown in Table IX,[26] where V, A, and S denote the vector, axial-vector, and scalar variants.

It should be borne in mind that the results given in Tables VIII and IX correspond to two independent experiments. In Table IX the minimum hadron energy has been increased to 12 GeV, and the CC distribution is normalized to the particles whose path length was large enough to allow them to pass through at least 15 steel blocks. Assuming a definite variant of the 4-fermion interaction and knowing R_ν, the value of $R_{\bar{\nu}}$ can be determined in the framework of the quark-parton model. When this quantity is compared with its experimental value, the $V+A$ variant is definitely excluded, but there is also disagreement for the pure $V-A$ variant. In view of the possible systematic errors, the authors do not consider the problem of finding the optimum mixture of V and A.

The results for the energy distribution of the hadrons,

TABLE VIII. The Caltech-Fermilab inclusive experiment (1974).

Path length, m	ν		$\bar{\nu}$	
	Observed	CC estimate	Observed	CC estimate
$1.4-\infty$	666	666 (assumption)	444	444 (assumption)
1.4—6.0	371	412	207	171
0—1.4	332	155	202	41
R	$\frac{177}{321}=0.22$		$\frac{161}{485}=0.33$	
$\left(\frac{\sigma_{\bar{\nu}}}{\sigma_\nu}\right)_{NC}$	0.5			

TABLE IX. The Caltech-Fermilab inclusive experiment (1975).

Variant of the weak interaction	R_ν	$R_{\bar{\nu}}$	$R_{\bar{\nu}}$, calculated from R_ν	$\left(\frac{\sigma_{\bar{\nu}}}{\sigma_\nu}\right)_{NC}$
Measured (E_{had} >12 GeV)	0.21	0.43	—	0.7
$V-A$	0.23	0.53	0.23	0.8
$V+A$	0.37	0.38	3.33	1.0
S	0.18	0.24	0.54	0.5

shown in Figs. 8 and 9, are also of interest. Figure 8a demonstrates the correctness of the assumption that the particles passing through more than 14 scintillation counters correspond to CCs, i.e., that they are muons. Figure 8b exhibits an appreciable enhancement of the experimental points in relation to the curve calculated for CCs. Assuming that this enhancement is due to NCs, the authors obtained the distribution of NC events with respect to E_{had} which is shown in Fig. 8c. This distribution agrees best with the $V-A$ variant, but it is also consistent with both the $V+A$ and S variants. A more definitive picture is observed in Fig. 9 for the NC $\bar{\nu}$ events. The curves in this figure are obtained by calculating distributions analogous to those of Fig. 8. We see that the $V+A$ variant is definitely excluded, while the S variant appears to be somewhat worse than the $V-A$ variant.

D. Inclusive processes involving charged currents

All the experiments discussed in the preceding subsections involved a determination of the value of R,

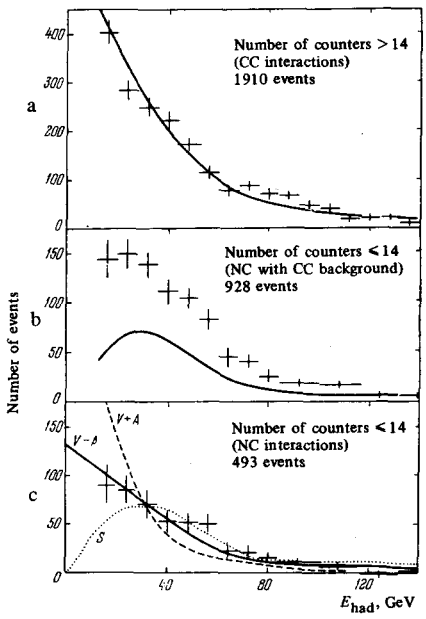

FIG. 8. Energy distribution of the hadrons in the 1975 neutrino experiment of the Caltech-Fermilab group. a) Events with a long-range particle passing through more than 14 counters (the curve shows the calculated result for CCs); b) events with no long-range particles (the curve shows the calculated result for CCs); c) the distribution for NC events obtained by subtraction in case b (the curves are given for the $V-A$, $V+A$, and S variants of the weak interaction involving NCs).

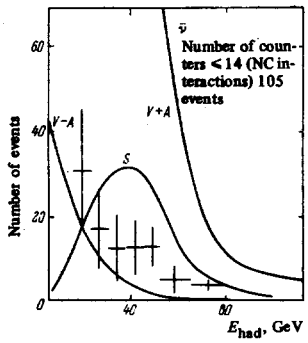

FIG. 9. Energy distribution of the hadrons in the 1975 antineutrino experiment of the Caltech-Fermilab group. The experimental data for NCs are obtained as in Fig. 8. The curves for the $V-A$, $V+A$, and S variants are normalized to the data of the neutrino experiment (see Fig. 8).

i.e., a comparison of the NC and CC cross sections. Before discussing the results for the neutral currents, we shall therefore say something about the main characteristics of inclusive processes involving neutral currents.

1) The cross sections for these reactions, measured by the same CERN-Gargamelle, HPW, and Caltech-Fermilab groups, rise linearly with energy, as can be seen from Figs. 10 and 11, taken from the review of Cundy.[27] We can introduce coefficients α_ν and $\alpha_{\bar\nu}$ by writing

$$\begin{aligned}\sigma(\nu_\mu+N\to\mu^-+\text{hadrons})&=\alpha_\nu E_\nu,\\ \sigma(\bar\nu_\mu+N\to\mu^++\text{hadrons})&=\alpha_{\bar\nu}E_{\bar\nu}.\end{aligned}\qquad(16)$$

The values of these coefficients are given in Table X. We see that they are energy-independent.

2) The $\bar\nu_\mu$ and ν_μ cross sections in (16) are in the ratio 1:3 over practically the whole of the studied energy range (Table X; the error in the ratio $\alpha_{\bar\nu}/\alpha_\nu$ is smaller than the errors in $\alpha_{\bar\nu}$ or α_ν individually, since a number of uncertainties drop out of this ratio). The value $\alpha_{\bar\nu}/\alpha_\nu=1/3$ is characteristic of a pure $V-A$ interaction. The parton-quark model gives the following expressions for α_ν and $\alpha_{\bar\nu}$ (if $\cos\theta_C$ is approximated by unity)[34]:

$$\begin{aligned}\alpha_\nu&=\frac{G^2m_N}{\pi}\left(Q+\frac{1}{3}\bar Q\right),\\ \alpha_{\bar\nu}&=\frac{G^2m_N}{\pi}\left(\frac{1}{3}Q+\bar Q\right),\end{aligned}\qquad(17)$$

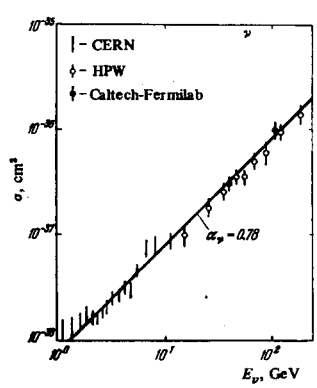

FIG. 10. The inclusive cross section for the process $\nu_\mu+N\to\mu^-+$hadrons as a function of energy.

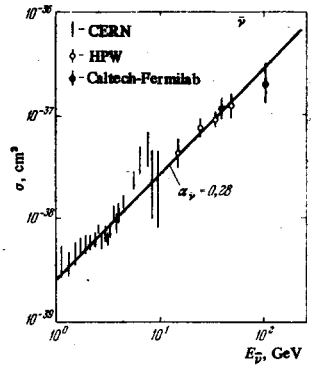

FIG. 11. The inclusive cross section for the process $\bar\nu_\mu+N\to\mu^++$hadrons as a function of energy.

where Q and $\bar Q$ denote the average fractions of the momentum of the initial nucleon carried away by the quarks or antiquarks. (Equation (17) is valid only if the target consists of equal numbers of protons and neutrons; this condition is satisfied with good accuracy in the actual experiments, since the targets are light nuclei.)

According to (17)

$$\frac{\alpha_{\bar\nu}}{\alpha_\nu}-\frac{1}{3}=\frac{8}{9}\frac{\bar Q/Q}{1+(\bar Q/3Q)}.\qquad(18)$$

The small value of the left-hand side of (18) implies that the antiquarks carry away a very small momentum, i.e., that the ratio $\bar Q/Q$ is much smaller than unity. The experimental values of $\bar Q/Q$, shown in the last column of Table X, are of order 0.05. However, it should be borne in mind that scaling may be violated at small values of q^2, the square of the momentum transferred from the neutrino to the muon. The value of $\bar Q/Q$ is approximately doubled if the appropriate corrections are introduced in this region. According to the CERN results, for example, $\bar Q/Q=0.10\pm0.03$.[35]

3) It should be pointed out that the strict linearity of the cross sections in Figs. 10 and 11 is in conflict with the so-called vector model of the weak interaction, which has recently been rather popular.[36–38] This model postulates the existence of at least three new quarks with relatively large effective masses. The cross sections should increase in crossing the thresholds for producing the new hadrons containing such quarks. In other words, it is natural to expect the cross sections (16) to have more than a linear growth with energy in the model of[36–38].

TABLE X. Characteristics of processes involving neutral currents.

Group	Energy region, GeV	α_ν	$\alpha_{\bar\nu}$	$\alpha_{\bar\nu}/\alpha_\nu$	$\bar Q/Q$
		10^{-38} cm²/GeV			
CERN[28,29]	1—10	0.76±0.02	0.28±0.03	0.38±0.02	0.05±0,02
HPW[30,31]	5—200	0.70±0.18	0.28±0.09	0.41±0.11	0.08±0.12
Caltech-Fermilab[32,33]	20—150	0.83±0.11	0.28±0.055	0.33±0.08	0.00±0,09

TABLE XI. Summary of inclusive results.

Group	Energy, GeV	R_ν	$R_{\bar\nu}$	$\left(\frac{\sigma_{\bar\nu}}{\sigma_\nu}\right)_{NC}$
CERN	1—10	0.217±0.026	0.55±0.07	0.96±0.18
HPW	5—200	0.12±0.04	0.32±0.08	1.09±0.53
Caltech-Fermilab	20—200	0.2—0.3	0.3—0.5	0.5—0.9

E. What can we learn from inclusive experiments?

The data on neutral currents obtained in the three experiments discussed in the preceding subsections are reproduced in Table XI. The following conclusions can be drawn from these data.

1) The values of R_ν and $R_{\bar\nu}$ have little or no variation with energy. This fact is also illustrated by Fig. 12; it can be seen that the three pairs of values of R_ν and $R_{\bar\nu}$ are rather similar. Thus the inclusive cross section for processes due to neutral currents rises linearly with energy, as in the case of charged currents.

2) According to (12) and (16), the ratio of the inclusive NC cross sections for neutrinos and antineutrinos is given by

$$\left(\frac{\sigma_{\bar\nu}}{\sigma_\nu}\right)_{NC}=\frac{\sigma(\bar\nu_\mu+N\to\bar\nu_\mu+\text{hadrons})}{\sigma(\nu_\mu+N\to\nu_\mu+\text{hadrons})}=\frac{R_{\bar\nu}}{R_\nu}\frac{\alpha_{\bar\nu}}{\alpha_\nu}. \tag{19}$$

The experimental values of $(\sigma_{\bar\nu}/\sigma_\nu)_{NC}$ in the last column of Table XI are close to unity. This may mean that only a single vector or axial-vector variant is present (or dominates) in the weak interaction involving NCs. If this is the case, the neutral currents conserve spatial parity. On the other hand, the situation may be different; for example, in the Weinberg-Salam model, which involves both variants, the same result holds for light nuclei with $Z\approx A/2$ for the reasonable value $\sin^2\theta_W = 1/2$ (see Eq. (26) below).

3) The distributions with respect to E_{had} shown in Figs. 4, 8, and 9 constitute evidence against the $V+A$ variant of the weak interaction involving NCs, but are more or less in agreement with the $V-A$ variant. In other words, if the neutral currents contain both vector and axial-vector components, the corresponding constants are of opposite sign. The data on the spectra are so far insufficient to determine the relative V and A contributions.

4) The experimental values of R_ν and $R_{\bar\nu}$ are in agreement with the predictions of both the Weinberg model and the vector model of the weak interaction. This point is discussed in more detail in the next two subsections.

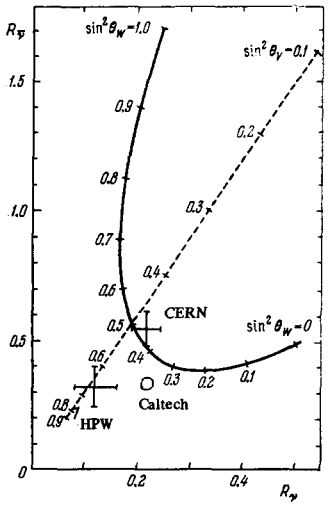

FIG. 12. The experimental values of R_ν and $R_{\bar\nu}$. The solid curve is the calculated result in the quark-parton version of the Weinberg-Salam model (Eq. (26)), and the dashed line corresponds to the vector model (Eq. (41)).

F. Neutral currents in the Weinberg-Salam model

In the Weinberg-Salam model,[14,15] the neutral weak current has the structure

$$J_\alpha^Z=J_\alpha^3-2\sin^2\theta_W J_\alpha^{em}, \tag{20}$$

where θ_W is a free parameter of the model known as the Weinberg angle, J_α^{em} is the ordinary electromagnetic current, and J_α^3 is the third isotopic component of the weak $V-A$ current, whose components are expressed in the following form in terms of the operators of the quarks

$q=\begin{pmatrix}u\\ d_C\end{pmatrix}$ and the leptons $E=\begin{pmatrix}\nu_e\\ e\end{pmatrix}$ and $M=\begin{pmatrix}\nu_\mu\\ \mu\end{pmatrix}$:

$$J_\alpha^i=\left[\bar q\frac{\tau_i}{2}\gamma_\alpha(1+\gamma_5)q\right]+\left[\bar E\frac{\tau_i}{2}\gamma_\alpha(1+\gamma_5)E\right]+\left[\bar M\frac{\tau_i}{2}\gamma_\alpha(1+\gamma_5)M\right]. \tag{21}$$

If the charged currents are defined as

$$J_\alpha^\pm=J_\alpha^1\pm iJ_\alpha^2, \tag{22}$$

the effective Lagrangian of the weak interaction is the same as (4) except for the addition of the neutral current

$$\mathcal{H}_W=\frac{G}{\sqrt2}(J_\alpha^+J_\alpha^-+J_\alpha^ZJ_\alpha^Z). \tag{23}$$

It should be borne in mind here that the product of distinct terms in the last expression appears with a coefficient 2; in particular, neutrino-hadron interaction processes correspond to the expression

$$\frac{G}{\sqrt2}[\bar\nu\gamma_\alpha(1+\gamma_5)\nu]\left\{\bar q\gamma_\alpha\left[\tau_3\frac{1+\gamma_5}{2}-2\sin^2\theta_W\frac{\tau_3+(1/3)}{2}\right]q\right\}. \tag{24}$$

The values which follow from (24) for the vector and axial-vector coupling constants g_V and g_A in units of $G/\sqrt2$ are shown in Table XII, where for completeness

TABLE XII. Values of the vector and axial-vector coupling constants for valence quarks.

Current	Model	Constant	$\nu_\mu u$	$\nu_\mu d$
NC	Weinberg-Salam model	g_V	$\frac12-\frac43\sin^2\theta_W$	$-\frac12+\frac23\sin^2\theta_W$
		g_A	$-\frac12$	$\frac12$
	Vector model	g_V	$1-\frac43\sin^2\theta_V$	$-1+\frac23\sin^2\theta_V$
		g_A	0	0
CC	Reactions $\nu_\mu d\to\mu^-u$, $\bar\nu_\mu u\to\mu^+d$	g_V	1	1
		g_A	−1	−1

we also give the values of g_V and g_A for the case of transitions involving CCs with $\cos\theta_C$ negligibly different from 1. In the quark-parton model, the inclusive cross sections for processes involving neutrino or antineutrino interactions with nucleons are determined by the elastic lepton-quark interaction. The cross section for such an interaction can be expressed in terms of definite combinations of g_V and g_A:

$$\begin{aligned}\sigma_\nu &\sim g_V^2+g_A^2-g_Vg_A,\\ \sigma_{\bar\nu} &\sim g_V^2+g_A^2+g_Vg_A.\end{aligned} \tag{25}$$

If only the "valence" quarks are taken into account (the role of the "sea" of quark-antiquark pairs is characterized by the quantity $\bar Q/Q$ in Table X, which is small experimentally), it is easy to obtain the ratio of the cross sections involving NCs and CCs for a target consisting of arbitrary proportions of u and d quarks. So far, inclusive experiments have been carried out mainly for relatively light nuclei containing roughly equal numbers of protons and neutrons and hence also roughly equal numbers of u and d quarks. In this case,[39,40]

$$R_\nu=\frac12-\sin^2\theta_W+\frac{20}{27}\sin^4\theta_W,\quad R_{\bar\nu}=\frac12-\sin^2\theta_W+\frac{20}{9}\sin^4\theta_W,$$
$$\left(\frac{\sigma_{\bar\nu}}{\sigma_\nu}\right)_{\rm NC}=\frac13\frac{R_{\bar\nu}}{R_\nu}. \tag{26}$$

The curve in Fig. 12, calculated according to Eqs. (26), is in agreement with the data of inclusive experiments if the Weinberg angle lies in the range

$$\sin^2\theta_W=0.45\pm0.10. \tag{27}$$

There is another possible method of estimating R_ν and $R_{\bar\nu}$, which does not make use of any parton-model hypothesis but in which the qualities (26) are replaced by inequalities.[41,42] The scheme of deriving such inequalities is quite simple. The cross section for any process which takes place in the presence of a neutrino-nucleon interaction is determined by the square of a matrix element of the hadronic current. The ratio of the cross sections for such processes involving neutral and charged currents is therefore given by

$$R_\nu=\frac{\sigma(\nu_\mu+N\to\nu_\mu+X)}{\sigma(\nu_\mu+N\to\mu^-+X')}=\frac{|\langle X|j^3-2\sin^2\theta_W j^{em}|N\rangle|^2}{|\langle X'|j^1+ij^2|N\rangle|^2}, \tag{28}$$

where X and X' are similar hadron states, say $n+\pi^+$ and $p+\pi^+$,

$$j^i=l_\alpha J^i_\alpha,\qquad j^{em}=l_\alpha J^{em}_\alpha, \tag{29}$$

and l_α is a leptonic matrix element, which is the same for both neutral and charged currents if the muon mass is neglected.

Now introducing the notation

$$\begin{aligned}&\sigma^-=\sigma(\nu_\mu+N\to\mu^-+X'),\quad \sigma^+=\sigma(\bar\nu_\mu+N\to\mu^++X'),\\ &V^{em}=\frac{G^2}{4\pi^2\alpha^2}\int dQ^2Q^4\frac{d\sigma(e^-+N\to e^-+X)}{dQ^2},\end{aligned} \tag{30}$$

and using the fact that

$$\begin{aligned}&\sigma^\pm\sim|\langle X'|j^\pm|N\rangle|^2=2|\langle X|j^3|N\rangle|^2,\\ &V^{em}\sim|\langle X|j^{em}|N\rangle|^2,\end{aligned} \tag{31}$$

as well as the inequality

$$a^*b+ab^*\leqslant2\sqrt{|a|^2|b|^2}, \tag{32}$$

we obtain the following lower bound on R_ν:

$$R_\nu\geqslant\frac12\left(1-2\sin^2\theta_W\right)\sqrt{\frac{V^{em}}{\sigma^-}}\Big)^2. \tag{33}$$

Similarly, we can derive a bound on $R_{\bar\nu}$:

$$R_{\bar\nu}=\frac{\sigma(\bar\nu_\mu+N\to\bar\nu_\mu+X)}{\sigma(\bar\nu_\mu+N\to\mu^++X')}\geqslant\frac12\left(1-2\sin^2\theta_W\right)\sqrt{\frac{V^{em}}{\sigma^+}}\Big)^2. \tag{34}$$

The inequalities (33) and (34) hold for transitions into completely well-defined states X and X' as well as for the sums of cross sections. In particular, they can be written for the total cross sections.[42] In that case,

$$V^{em}_{\rm tot}=\frac{G^2}{4\pi^2\alpha^2}\int Q^4\frac{d\sigma(ep)}{dQ^2}dQ^2=\frac{G^2}{\pi}\frac43ME\int F_2(x)\,dx, \tag{35}$$

where M is the nucleon mass, $x=Q^2/2M\nu$ is the Bjorken variable for deep inelastic ep scattering (ν is the energy of the virtual photon in the laboratory system), and $F_2(x)=\nu W_2$ is a certain structure function. Experimentally, it is found that

$$\begin{aligned}&\int F_2(x)\,dx=0.14\pm0.02,\\ &\sigma^-_{\rm tot}=\frac{G^2}{\pi}ME(0.52\pm0.11),\\ &\sigma^+_{\rm tot}=\frac{G^2}{\pi}ME(0.19\pm0.22),\end{aligned}\Bigg\} \tag{36}$$

from which

$$\begin{aligned}&\frac{V^{em}_{\rm tot}}{\sigma^-_{\rm tot}}=0.36\pm0.05,\\ &\frac{V^{em}_{\rm tot}}{\sigma^+_{\rm tot}}=1.0\pm0.1.\end{aligned} \tag{37}$$

The curve which determines the lower bounds on R_ν and $R_{\bar\nu}$ according to (33), (34), and (37) lies much lower than the "parton" curve shown in Fig. 12. On the other hand, such inequalities are useful in considering processes involving single pion production.

G. Neutral currents in the "vector" model

By introducing new quarks, the authors of[36-38] were able to construct a theory which includes particles with both left-handed and right-handed polarizations. The neutral current for the quarks (and hence for the hadrons) has a pure vector character in such a theory. Although the "vector" model encounters major theoretical difficulties, it has recently been discussed rather widely. In this connection, it seems appropriate to examine the predictions of the model for processes involving neutral currents.

The weak interaction in the vector model has the structure (23), but the current J^3_α which appears in (20) is different from that of (21):

$$J_\alpha^3 = \sum_q (\bar{q}\tau_3\gamma_\alpha q) + \left(\bar{\nu}_e\gamma_\alpha \frac{1+\gamma_5}{2}\nu_e\right) + \left(\bar{\nu}_\mu\gamma_\alpha \frac{1+\gamma_5}{2}\nu_\mu\right) - (\bar{e}\gamma_\alpha e) - (\bar{\mu}\gamma_\alpha\mu) + \ldots \quad (38)$$

The dots here refer to the contributions of additional leptons, and the summation is taken over all possible "types" of quarks. In addition, the Weinberg angle θ_W is replaced by another parameter, which we shall denote by θ_V. Finally, the authors of[36-38] consider that it is possible to dispense with the usual Higgs scheme of spontaneous symmetry breaking, and they insert a coefficient $\varkappa$ in front of the product $J_\alpha^Z J_\alpha^Z$ in (23), this coefficient being expressed in terms of θ_V and the masses of the vector bosons $W^\pm$ and Z^0:

$$\varkappa = \frac{1}{\cos^2\theta_V}\frac{M_W^2}{M_Z^2}. \quad (39)$$

On the other hand, a comparison with the experimental data in[38] favors a value of $\varkappa$ close to unity. We therefore put $\varkappa = 1$ in what follows.

If the quarks have only a vector interaction in the neutral current, then the cross sections for neutrino and antineutrino interactions involving NCs are equal:

$$\left(\frac{\sigma_{\bar{\nu}}}{\sigma_\nu}\right)_{NC} = 1. \quad (40)$$

As we have already pointed out, this equality is in agreement with the experimental data given in Table XI. This fact is perhaps the greatest success of the vector model.

The values of the weak-interaction coupling constants for the quarks which follow from (20), (23), and (38) are shown in Table XII. Substituting these values in (25), we find the following values of R_ν and $R_{\bar{\nu}}$ for the inclusive cross sections involving NCs and CCs (below the threshold for producing the new quarks) in the case of a target consisting of equal numbers of protons and neutrons:

$$R_{\bar{\nu}} = 3R_\nu = 2 - 4\sin^2\theta_V + \frac{20}{9}\sin^4\theta_V. \quad (41)$$

The predictions of the vector model are shown by the dashed line in Fig. 12. We see that agreement with the

TABLE XIII. Experimental arrangements for studying exclusive events using a beam of muonic neutrons.

Laboratory	Substance in the chamber	Chamber dimensions	Effective volume
Argonne	Hydrogen, deuterium	12 ft, 20 m^3	11 m^3
CERN	Propane C_3H_8	1.2 m, 1 m^3	0.5 m^3
CERN	Freon CF_3Br	8 m^3	3 m^3
Brookhaven	Hydrogen, deuterium	7 ft	5 m^3
Brookhaven	Aluminum*	26 tons	8 tons
Batavia	Hydrogen, deuterium	12 ft, 26 m^3	21 m^3
CERN (Aachen-Padua)	Aluminum**	30 tons	

*26 modules of aluminum optical spark chambers and scintillation counters.
**129 modules of aluminum optical spark chambers and 12 iron plates of thickness 4 cm.

TABLE XIV. Searches for elastic neutrino-proton scattering.

Group	CERN[43]	CERN[44]	Argonne[45]
Chamber	Propane	Freon	Deuterium
Selection criteria (E_ν in GeV, t in GeV^2)	$1 < E_\nu < 4$, $0.3 < \lvert t\rvert < 1$	$1 < E_\nu < 5$, $0.3 < \lvert t\rvert$	$0.7 < E_\nu$, $0.43 < \lvert t\rvert$, $216° < \varphi < 324°$
Process	$\nu_\mu + p \to \nu_\mu + p$	$\nu_\mu + p \to \nu_\mu + p$	$\nu_\mu + p \to \nu_\mu + p$
Number of events	2	2	4 (background 4.91 ± 2.44)
$\frac{\sigma(\nu_\mu + p \to \nu_\mu + p)}{\sigma(\nu_\mu + n \to \mu^- + p)}$ measured with	0.12 ± 0.06		-0.08 ± 0.20
$\frac{\sigma(\nu_\mu + p \to \nu_\mu + p)}{\sigma(\nu_\mu + n \to \mu^- + p)}$ 90% confidence	< 0.22	< 0.77	< 0.32

CERN experimental data is achieved for $\sin^2\theta_V \sim 0.5$, whereas the data of the HPW group correspond to $\sin^2\theta_V \sim 0.6$–0.7.

4. EXCLUSIVE EXPERIMENTS

A. Experiment

In this section we discuss the exclusive processes enumerated in (11). Only one of these processes, namely the reaction $\bar{\nu}_e + d \to \bar{\nu}_e + p + n$, was studied using a beam of electronic antineutrinos from a reactor. All the other experiments were performed using a beam of muonic neutrinos from an accelerator. The characteristics of the detectors for analyzing the exclusive events in the ν_μ beam (as a rule, bubble chambers) are given in Table XIII.

B. The elastic scattering process $\nu_\mu + p \to \nu_\mu + p$

Experiments have been carried out using propane and freon chambers at CERN and a hydrogen chamber at Argonne.[43-45] The principal difficulty was the presence of a neutron background, since the process $n + p \to n + p$ also leads to a single proton. To reduce the background, events were selected within a definite range of neutrino energies and momenta transferred to the proton. The results are shown in Table XIV. It should be noted that the data of[44] are preliminary.

So far, no elastic $\nu_\mu p$ or $\bar{\nu}_\mu p$ scattering has been detected, but the experiments are not yet accurate enough for this.

From the theoretical point of view, elastic neutrino-proton scattering is of interest because its cross section can be expressed in terms of the nucleon form factors, which are known with good accuracy. Introducing the elastic (G_E), magnetic (G_M), and axial-vector (G_A) form factors of the neutral current, the differential cross section can be expressed in terms of these quantities by means of a relation similar to the well-known Rosenbluth formula for ep scattering, but with an additional axial-vector form factor[46-48]:

$$\frac{d\sigma}{dQ^2} = \frac{G^2}{2\pi}\left[\left(\frac{G_E^2 + \tau G_M^2}{1+\tau} + G_A^2\right)\left(1 - \frac{Q^2}{2ME_\nu} - \frac{Q^2}{4E_\nu^2}\right) + \frac{Q^2}{2ME_\nu}\left\{\frac{M}{E_\nu}[\tau G_M^2 + (1+\tau)G_A^2] \mp \left(1 - \frac{Q^2}{4ME_\nu}\right)2G_M G_A\right\}\right], \quad (42)$$

where Q is the momentum of the recoil proton in the laboratory system, M is the proton mass, and

$$\tau = \frac{Q^2}{4M^2}; \quad (43)$$

the signs ∓ refer to νp and $\bar{\nu} p$ scattering, respectively. If the muon mass is neglected, the foregoing equations are also valid for the processes $\nu_\mu + n \to \mu^- + p$ and $\bar{\nu}_\mu + p \to \mu^+ + n$ involving CCs; the only difference is in the values of the coupling constants.

In the Weinberg-Salam model[49] for the neutral currents,

$$\left.\begin{aligned} G_M &= [(1-4\sin^2\theta_W)\mu_p - \mu_n] F_V(Q^2), \\ G_E &= \{1-4\sin^2\theta_W - \tau[(\mu_p-1)(1-4\sin^2\theta_W) - \mu_n]\} F_V(Q^2), \\ G_A &= -1.25 F_A(Q^2); \end{aligned}\right\} \quad (44)$$

it is assumed here that all the vector form factors have the same Q^2 dependence. Both F_V and F_A are normalized to unity at $Q^2 = 0$. The value $G_A(0) = -1.25$ is determined experimentally from the β decay of the neutron.

In the vector model,[36]

$$\left.\begin{aligned} G_M &= 2[(1-2\sin^2\theta_V)\mu_p - \mu_n] F_V(Q^2), \\ G_E &= 2\{1-2\sin^2\theta_V - \tau[(\mu_p-1)(1-2\sin^2\theta_V) - \mu_n]\} F_V(Q^2), \\ G_A &= 0. \end{aligned}\right\} \quad (45)$$

Using the experimental limits on $\sigma_{\nu p}$ given in Table XIV, the foregoing equations enable us to obtain the following bounds on θ_W and θ_V:

$$\begin{aligned} \sin^2\theta_W &< 0.5, \\ \sin^2\theta_V &< 0.9. \end{aligned} \quad (46)$$

The expression for the ratio of the cross sections for elastic scattering involving NCs and CCs simplifies at high energy, since the form factors provide a cutoff in Q^2 at values much less than ME_ν or E_ν^2. In this case, scattering occurs practically only in the forward direction, so that[50]

$$\frac{\sigma(\nu p \to \nu p)}{\sigma(\nu n \to \mu^- p)} = \frac{\sigma(\bar{\nu} p \to \bar{\nu} p)}{\sigma(\bar{\nu} p \to \mu^+ n)} \approx \frac{1}{4}\,\frac{g_A^2 + g_V^2}{1.25^2 + 1} = \frac{g_A^2 + g_V^2}{10.25}, \quad (47)$$

where g_A and g_V are the values of the form factors G_A and G_E at $Q^2 = 0$. The relation (47) is convenient for estimating the admissible values of the angles θ_W and θ_V.

C. Single pion production

The following processes involving neutral currents are possible:

$$\left.\begin{aligned} &\nu_\mu + p \to \nu_\mu + n + \pi^+, \\ &\nu_\mu + p \to \nu_\mu + p + \pi^0, \\ &\nu_\mu + n \to \nu_\mu + n + \pi^0, \\ &\nu_\mu + n \to \nu_\mu + p + \pi^-. \end{aligned}\right\} \quad (48)$$

These processes are to be compared with those due to charged currents:

$$\left.\begin{aligned} &\nu_\mu + p \to \mu^- + p + \pi^+, \\ &\nu_\mu + n \to \mu^- + p + \pi^0, \\ &\nu_\mu + n \to \mu^- + n + \pi^+. \end{aligned}\right\} \quad (49)$$

Experiments have been carried out using a 12-ft chamber at Argonne filled with hydrogen or deuterium,[45,51,52] propane[53-55] and freon[20,56,57] chambers at CERN, and a 7-ft chamber at Brookhaven.[58] Experiments have also been performed at Brookhaven[59,60] and CERN[61] using aluminum spark chambers. The statistics of all these experiments are shown in Table XV. Unfortunately, the number of events is relatively large only for the experiments using nuclei, which are difficult to interpret because of the charge-exchange processes involving transitions of charged pions into neutral pions. Very few neutrino events have been seen so far in the experiments using hydrogen or deuterium targets.

The results for the ratio NC/CC are shown in Table XVI. The transition from Table XV to Table XVI is non-trivial in certain cases, as it requires allowance for various corrections. It can be seen that, within the very large errors, the data of the various experiments are in mutual agreement. There is only a single serious discrepancy between the data in the fourth and fifth lines of Table XVI. These data can be brought into agreement only if it is assumed that $\sigma(\nu_\mu n \to \nu_\mu n \pi^0) \gg \sigma(\nu_\mu p \to \nu_\mu p \pi^0)$, but it seems unlikely that this inequality is valid. The value given in the fourth line of the table appears to be the less reliable one, having been obtained from older data.[53]

On the other hand, the Argonne experiment[65,66] yielded 119^{+12}_{-16}, 44 ± 9, and 43.7 ± 11 CC events for the reactions $\nu_\mu + p \to \mu^- + p + \pi^+$, $\nu_\mu + n \to \mu^- + p + \pi^0$, and $\nu_\mu + n \to \mu^- + n + \pi^+$, respectively,[1)] and hence

$$\begin{aligned} \frac{\sigma(\nu_\mu n \to \mu^- p\pi^0) + \sigma(\nu_\mu n \to \mu^- n\pi^+)}{\sigma(\nu_\mu p \to \mu^- p\pi^+)} &= 0.74^{+0.14}_{-0.16}, \\ \frac{\sigma(\nu_\mu n \to \mu^- n\pi^+)}{\sigma(\nu_\mu n \to \mu^- p\pi^0)} &= 1.01 \pm 0.33. \end{aligned} \quad (50)$$

If these ratios are used to express the denominators of the fourth and fifth lines of Table XVI in terms of the same cross section $\sigma(\nu_\mu + p \to \mu^- + p + \pi^+)$ as in the first three lines, the corresponding values must be reduced by about a factor of three. In this case, the entire set of data in the lower half of Table XVI (lines 3, 4, and 5) become inconsistent, although the experimental errors are of course very large.

It should be borne in mind, however, that the experiments of[20,61] were carried out with nuclei. This makes it difficult to interpret their results. Adler *et al.*[64] showed that the nuclear effects lead to an effective reduction of the ratio $\sigma(\nu_\mu N \to \nu_\mu N \pi^0)/\sigma(\nu_\mu n \to \mu^- p \pi^0)$ by about a factor of two. In other words, the quantities given in lines 4–6 of Table XVI should be multiplied by 1.5–2 when comparisons are made with data obtained using hydrogen or deuterium.

Experiments on single pion production are of special interest, as they can provide information about the isotopic structure of the neutral current. Unfortunately, the ratio of the cross sections for the processes $\nu_\mu p \to \nu_\mu p \pi^0$ and $\nu_\mu p \to \nu_\mu n \pi^+$ was determined with very poor accuracy in the Argonne experiment[45,51,52]:

[1)] Assuming that the charged current satisfies the $\Delta I = 1$ rule, i.e., that there is no $\Delta I = 2$ component, these data correspond to a ratio of the amplitudes A_1 and A_3 for producing final states with $I = 1/2$ and $I = 3/2$ given by $A_1/A_3 = (0.78^{+0.13}_{-0.17}) \times \exp(i\varphi)$, with $\varphi = (92^{+10}_{-11})°$.[65,66]

TABLE XV. Numbers of events and selection criteria in experiments on single pion production.

Reaction		$\nu p \to \nu n \pi^+$	$\nu p \to \nu p \pi^0$	$\nu n \to \nu p \pi^-$	$\nu p \to \mu^- p \pi^+$	$\nu n \to \mu^- p \pi^0$	$\bar{\nu} N \to \bar{\nu} N \pi^0$	$\bar{\nu} p \to \mu^+ p \pi^-$
Argonne, hydrogen, deuterium[52]	Selection criteria:	$p_p < 1$ GeV/c; $p_\pi < 0.4$ GeV/c; π^+ moving upward; at least 20 cm to the track of a cosmic particle						
	Number of events:	8	8	25	?	...	...	...
	Background:	1.6 ± 0.8	2.0 ± 0.6	18 ± 7				
CERN, propane[55]	Selection criteria:	$p_\pi < 0.7$ GeV/c; charge is conserved in a "clean" event; slow protons are present in a "dirty" event						
	Number of "clean" events:	4	2	3	$\begin{cases} 50\pi^+ \\ 77p \\ 37p + \pi^+ \end{cases}$	...	...	...
	Number of "dirty" events:	5	1	0	$\begin{cases} 17\pi^+ \\ 33p \\ 14p + \pi^+ \end{cases}$	...	...	...
CERN, freon[57]	Observed events:	...	142 (together with $\nu n \to \nu n \pi^0$)	...	384	...	152	216
	With corrections:	...	146 ± 13	...	338 ± 27	...	176 ± 14	199 ± 15
Brookhaven, aluminum spark chambers[60]	Number of events:	...	123 (together with $\nu n \to \nu n \pi^0$)	...	...	356	...	...
Brookhaven, deuterium[58]	Number of events:	...	...	8	56	~ 17 ($\nu n \to \mu^- n \pi^+$)	...	...
Aachen-Padua, aluminum spark chambers[61]	Number of events:		124 (together with $\nu n \to \nu n \pi^0$)		145	67	56	

$$r \equiv \frac{\sigma(\nu_\mu + p \to \nu_\mu + p + \pi^0)}{\sigma(\nu_\mu + p \to \nu_\mu + n + \pi^+)} = 3.1 \pm 2.2. \qquad (51)$$

If the state with isospin $I = 3/2$ were dominant in the final state (in which case the neutral current would contain a large isovector component with $\Delta I = 1$), we would have $r = 2$; but if only isospin $I = 1/2$ were present, we would have $r = 1/2$. The experimental result is basically consistent with either possibility.

Valuable information can be gained by studying mass distributions of the $p + \pi$ system in order to observe the isospin-3/2 Δ resonance. The $p + \pi^-$ mass distribution in the reaction $\nu_\mu n \to \nu_\mu p \pi^-$ found in the Argonne experiment[52] is shown in Fig. 13. It is not clear from this figure what type of structure occurs near the $\Delta^0(m = 1232$ MeV) resonance. If there were actually no Δ resonance, this would mean that the neutral current

TABLE XVI. The ratio *NC/CC* in single-pion production processes.

Ratio of cross sections	Argonne, hydrogen, deuterium[52]	CERN, propane[55]	CERN, freon (68% confidence)[57]	Aachen-Padua, aluminum spark chambers[61]	Brookhaven, aluminum spark chambers[60]	Brookhaven deuterium[58]	Weinberg-Salam model[62-64]
$\frac{\sigma(\nu_\mu p \to \nu_\mu n \pi^+)}{\sigma(\nu_\mu p \to \mu^- p \pi^+)}$	0.13 ± 0.06	0.12 ± 0.04	...	...	...	...	0.08–0.26
$\frac{\sigma(\nu_\mu n \to \nu_\mu p \pi^-)}{\sigma(\nu_\mu p \to \mu^- p \pi^+)}$	0.07 ± 0.03*	0.06 ± 0.04	...	...	...	0.14 ± 0.04	0.09–0.18
$\frac{\sigma(\nu_\mu p \to \nu_\mu p \pi^0)}{\sigma(\nu_\mu p \to \mu^- p \pi^+)}$	0.40 ± 0.22	...	...	...	...	...	0.07–0.18
$\frac{\sigma(\nu_\mu p \to \nu_\mu p \pi^0) + \frac{1}{3}\sigma(\nu_\mu n \to \nu_\mu n \pi^0)}{\sigma(\nu_\mu n \to \mu^- p \pi^0)}$	...	0.07 ± 0.05	...	...	...	...	
$\frac{\sigma(\nu_\mu p \to \nu_\mu p \pi^0) + \sigma(\nu_\mu n \to \nu_\mu n \pi^0)}{2\sigma(\nu_\mu n \to \mu^- p \pi^0)}$	...	...	>0.10 <0.20	0.43 ± 0.15	0.17 ± 0.06	...	0.19 for $\sin^2\theta_W = 0.39$
$\frac{\sigma(\bar{\nu}_\mu p \to \bar{\nu}_\mu p \pi^0) + \sigma(\bar{\nu}_\mu n \to \bar{\nu}_\mu n \pi^0)}{2\sigma(\bar{\nu}_\mu p \to \mu^+ n \pi^0)}$	...	...	>0.26 <0.44	0.59 ± 0.20	...	...	

*Only six events for $\nu_\mu + n \to \nu_\mu + p + \pi^-$ with an upward momentum are taken into account.

contained no isovector component and hence that gauge theories like the Weinberg-Salam model have nothing to do with neutral currents in the weak interaction. However, it was found that the neutron background (from the reaction $nn \to np\pi^-$, as well as $nn \to d\pi^-$ and $nd \to dp\pi^-$) in the Argonne experiment was large, particularly in the up-down direction, owing to the presence of the apertures in the upper part of the chamber. Of the total of 25 events shown in Fig. 13, there are 19 events in which the $p\pi^-$ system is moving downward. It is quite likely that practically all these events are due to the background. The distribution of the remaining six events, in which the $p\pi^-$ system is moving upward, is shown by the cross-hatched histogram in Fig. 13. We see that these events are in fact concentrated near the Δ^0 resonance. Their average mass is 1260 ± 30 MeV.

Figure 14 shows the effective-mass distributions of the $p+\pi^0$ and $p+\pi^-$ systems which were determined in the CERN experiment[57] for both NCs and CCs. In each case, there is a conspicuous peak in the region of the Δ resonance. However, it is difficult to give a quantitative interpretation of these data, since the experiment was carried out using nuclei.

It is rather difficult to make a comparison of the experimental data on single pion production with the theoretical models. To do so, we must make use of the inequalities (33) and (34), which involve the quantity V^{em}, defined by (30) in terms of the electroproduction cross section. For a laboratory energy ~ 2 GeV, it is found that[67,68]

$$\left.\begin{aligned} V^{em}(p\to p\pi^0) &\approx 0.12\cdot 10^{-38}\ \text{cm}^2\\ V^{em}(p\to n\pi^+) &\approx 0.08\cdot 10^{-38}\ \text{cm}^2\\ \sigma(\nu_\mu p\to \mu^- p\pi^+) &= (0.74\pm 0.18)\cdot 10^{-38}\,\text{cm}^2 \end{aligned}\right\} \qquad (52)$$

Using these values in the inequality (33) for the ratio $\sigma(\nu_\mu n \to \nu_\mu p\pi^-) : \sigma(\nu_\mu n \to \mu^- p\pi^0)$, together with the Argonne data given in (50) and in Table XVI, according to which this ratio has the value

$$R = \frac{\sigma(\nu_\mu n\to \nu_\mu p\pi^-)}{\sigma(\nu_\mu p\to \mu^- p\pi^+)}\frac{\sigma(\nu_\mu p\to \mu^- p\pi^+)}{\sigma(\nu_\mu n\to \mu^- p\pi^0)} = 0.19\pm 0.09, \qquad (53)$$

and putting $V^{em}(p\to n\pi^+) \approx V^{em}(n\to p\pi^-)$ by virtue of the predominance of the isovector contribution in the electroproduction process,[67] we find

$$\sin^2\theta_W \geqslant \frac{1-\sqrt{2R}}{2}\sqrt{\frac{\sigma(\nu_\mu n\to \mu^- p\pi^0)}{\text{Im}(p\to n\pi^+)}} \geqslant 0.2. \qquad (54)$$

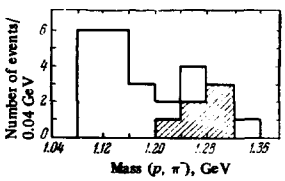

FIG. 13. The effective-mass distribution of the $p+\pi^-$ system found in the Argonne experiment.[52] The cross-hatched area gives the distribution for the events in which the $p\pi^-$ system is moving in the upward direction.

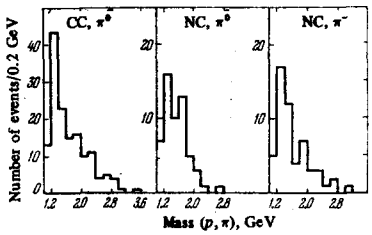

FIG. 14. The effective-mass distribution of the $p+\pi$ system found in the CERN experiment for reactions resembling $\nu_\mu + n \to \mu^- + p + \pi^0$, $\nu_\mu + p \to \nu_\mu + p + \pi^0$, and $\nu_\mu + n \to \nu_\mu + p + \pi^-$.[57]

Similarly, using the data of nuclear experiments[20,61] to determine the ratio $\sigma(\nu_\mu N \to \nu_\mu N\pi^0)/\sigma(\nu_\mu n \to \mu^- p\pi^0)$, assuming that the final state with $I = 3/2$ is dominant in processes involving CCs, and allowing for nuclear effects, the inequality (33) for the ratio[62]

$$\frac{\sigma(\nu_\mu p\to \nu_\mu p\pi^0)+\sigma(\nu_\mu n\to \nu_\mu n\pi^0)}{\sigma(\nu_\mu p\to \mu^- p\pi^+)+\sigma(\nu_\mu n\to \mu^- n\pi^+)-\sigma(\nu_\mu n\to \mu^- p\pi^0)} \qquad (55)$$

leads to the value[64]

$$\sin^2\theta_W \geqslant 0.35. \qquad (56)$$

As regards the vector model, the neutral weak current in this model contains no axial-vector component similar to the electromagnetic current. If, in addition, it is assumed that the isovector component is dominant in each case, the following set of relations can be derived[36]:

$$\begin{aligned} \sigma(\nu_\mu p\to \nu_\mu p\pi^0) &= \sigma(\nu_\mu n\to \nu_\mu n\pi^0)\\ &= 2\cos^4\theta_V\cdot V^{em}(p\to p\pi^0) = 0.24\cdot 10^{-38}\cos^4\theta_V,\\ \sigma(\nu_\mu p\to \nu_\mu n\pi^+) &= \sigma(\nu_\mu n\to \nu_\mu p\pi^-)\\ &= 2\cos^4\theta_V\cdot V^{em}(p\to n\pi^+) = 0.16\cdot 10^{-38}\cos^4\theta_V. \end{aligned} \qquad (57)$$

The quantities on the left-hand side can be determined from (52) and Table XVI, and $\sigma(\nu_\mu N \to \nu_\mu N\pi^0)$ must be multiplied by ~ 2.[64] The various ratios given in Table XVI correspond to values of θ_V in the range

$$0 \leqslant \sin^2\theta_V \leqslant 0.6. \qquad (58)$$

The errors here are still very large.

D. Multi-pion events

The 7-ft bubble chamber at Brookhaven was also used to study reactions involving the production of two or four pions.[58] The experimental results are shown in Table XVII. They yield the following value for the ratio

TABLE XVII. Multi-pion processes at Brookhaven.[58]

Type of events	Reaction	Target H_2	Target D_2
NC	$\nu_\mu p \to \nu_\mu \pi^+\pi^- p$	4	5
	$\nu_\mu p \to \nu_\mu \pi^+\pi^+\pi^-\pi^- p$	1	1
	$\nu_\mu n \to \nu_\mu \pi^+\pi^- n$	...	4
	Total events	15	
	Allowance for efficiency and background	23.1 ± 7.5	
CC + NC	Total number of multi-pion events	43	98
	Total multi-pion events	141 ± 12	
CC	Allowance for efficiency and background	100 ± 15	

TABLE XVIII. Strange-particle production by charged (SCC) and neutral (SNC) currents: the numbers of events.

Group	Argonne[52]		CERN[70,71]			
Technique, selection criteria	Hydrogen, deuterium; $p_\pi < 0.4$ GeV/c; $p_p < 1$ GeV/c		Freon; $E_{had} > 1$ GeV (for SNC); Λ or K_S^0 lifetime is less than $3\tau_\Lambda$ or $3\tau_{K_S^0}$			
Beam	ν_μ		ν_μ		$\bar{\nu}_\mu$	
Process	SNC	SCC	SNC	SCC	SNC	SCC
ΛK_S^0	1	1	0	1	1	3
ΛK^+	0	2	2	11	0	3
$K^0\bar{K}^0$	0	0	1	0	0	0
$K^+\bar{K}^0$	0	1	0	0	0	0
Λ	4	0	7	28	1	22
K_S^0	1	1	3	13	0	6
K^+	0	1	3	15	1	2
Total	6	6	16	68	3	33
With the same kinematics ($E_{had} > 1$ GeV)	6	2	16	48	3	11
Background	~1.5		~3			
$\frac{\text{SNC}}{\text{SCC}}$	~1		$0.34^{+0.17}_{-0.09}(\Delta S = 0)$ $\leq 0.024(\Delta S = 1)$		~0.3	

of the numbers of NC and CC events:

$$\frac{\sigma(\nu_\mu + N \to \nu_\mu + N + k\pi)}{\sigma(\nu_\mu + N \to \mu^- + N + k\pi)} = 0.23 \pm 0.08 \qquad (k \geqslant 2). \tag{59}$$

This value is in full agreement with the experimental ratio R_ν for inclusive processes (Table XI).

E. Strange-particle production

Experimental studies of strange-particle production were carried out at Argonne[52,69] and at CERN.[20,70,71] The detected particles were Λ, K_S^0, and K^+. The probability of detecting the particles $\Sigma^\pm$, Σ^0, or K^- was small. The results are shown in Table XVIII. It can be seen that different values were found for the ratio of the NC and CC cross sections for strange-particle production in the experiments at Argonne (~1) and at CERN (~1/3). The value found at CERN is in agreement with the overall ratio R_ν in Table XI. The value obtained by the Argonne group was based on very poor statistics and may change significantly. It should be pointed out that all six SNC candidates in the Argonne experiment correspond to processes involving "pure" production of ΛK_S^0, Λ, or K_S^0, whereas only two of the six SCC events have this property; the remaining events involve the production of non-strange hadrons p or π^- in addition to the strange particles. The ratio SNC/SCC for (exclusive) events of the same structure in the Argonne experiment is even greater than unity, therefore contradicting the CERN data, although it is true that the CERN experiment involved not a study of the exclusive production of a ΛK pair, but the inclusive production of strange particles. The absence of transitions with $\Delta S = \pm 1$ (see the last line of Table XVIII) is consistent with the absence of the decay $K^\pm \to \pi^\pm \bar{\nu}\nu$ in Table I.

The ratio SNC/SCC is of special interest in determining the weight with which the strange quarks appear in the neutral current. This problem has a direct bearing on the possible existence of a fourth "charmed" quark C.[72] In a theory involving "charm," the charged current (1) contains the additional term

$$(\bar{c}O_\alpha s_C), \tag{60}$$

where

$$O_\alpha = \gamma_\alpha(1 + \gamma_5),$$
$$\bar{s}_C = -d\sin\theta_C + s\cos\theta_C. \tag{61}$$

The term (60) has no effect on transitions between the ordinary hadrons, which contain no charmed quarks. At the same time, the neutral current now involves a term $(\bar{s}_C O_\alpha s_C)$, and this term has the structure (the plus and minus signs correspond to an isoscalar and isovector, respectively)

$$(\bar{u}O_\alpha u + \bar{c}O_\alpha c) \pm (\bar{d}_C O_\alpha d_C + \bar{s}_C O_\alpha s_C) = (\bar{u}O_\alpha u + \bar{c}O_\alpha c) \pm (\bar{d}O_\alpha d + \bar{s}O_\alpha s), \tag{62}$$

in which the strange quark s appears on an equal footing with the non-strange quarks u and d and the unwanted terms $(\bar{d}O_\alpha s)$ and $(\bar{s}O_\alpha d)$ are absent. The problem of what contribution the strange quarks make to the neutral current is therefore related to the possible existence of charmed particles.

This problem might be solved, for example, by looking for events involving a relatively small momentum transfer from the initial to the final neutrino. The vector-dominance model should evidently work in this case. If the neutral current actually has the structure (62), the φ meson should give a contribution to the same order as the ρ or ω mesons, so that the associated production of strange particles should be large, i.e., the ratio SNC/SCC should be larger than the "normal" value of order 0.2.

F. Neutrino-induced break-up of the deuteron

We have so far considered only processes involving muonic neutrinos. This is connected with the fact that such neutrinos can be obtained with a high energy from accelerators, and the weak-interaction cross sections rise with E_ν. A reactor can serve as a source of electronic antineutrinos, in which case they have low energies. It is for this reason that only a single experiment involving electronic antineutrinos has so far been carried out[73]; in this experiment, Reines *et al.* made an unsuccessful search for the reaction

$$\bar{\nu}_e + d \to \bar{\nu}_e + p + n. \tag{63}$$

The cross section for this reaction was calculated in[74,75], where allowance was made for the experimental antineutrino spectrum (events with $E_{\bar{\nu}} = 2.2$–5 MeV were selected in the experiment). In terms of the Weinberg-Salam model, the theoretical cross section was found to have the completely well-defined value[75] 4.4×10^{-45} cm^2. The current experimental upper limit exceeds this value by a factor of six, i.e., by three standard deviations[73]:

$$\sigma(\bar{\nu}_e + d \to \bar{\nu}_e + p + n) < 25 \cdot 10^{-45} \text{ cm}^2. \tag{64}$$

G. What can we learn from exclusive experiments?

The following conclusions can be drawn from the experimental results discussed in the preceding subsections:

TABLE XIX. Neutrino-electron scattering.

Process	$\nu_\mu e^- \to \nu_\mu e^-$	$\bar{\nu}_\mu e^- \to \bar{\nu}_\mu e^-$	$\nu_e e^- \to \nu_e e^-$	$\bar{\nu}_e e^- \to \bar{\nu}_e e^-$
Neutrino energy	1–10 GeV			0–7 MeV
Selection criteria	0.3 GeV $\leqslant E_e$, $\theta_e \leqslant 5°$		1 GeV $\leqslant E_e$, $\theta_e \leqslant 4°$	3.2 MeV $\leqslant E_e$ $\leqslant 4.5$ MeV
Photographs analyzed	375 000	970 000		
Observed single e^-	0	3	$\leqslant 1$	0.77 ± 0.33 per day
Estimated background		0.52 ± 0.21		< 0.05 per day
Limits on cross sections, cm^2/GeV	σ/E_ν $\leqslant 2.6 \cdot 10^{-42}$ (90% confidence)	$0.3 \cdot 10^{-42}$ $\leqslant \sigma/E_\nu$ $\leqslant 2.9 \cdot 10^{-42}$ (90% confidence)	σ/E_ν $\leqslant 7 \cdot 10^{-40}$ $= 40\sigma_{FG}/E_\nu$	$\sigma/E_\nu = (0.8 \pm 0.4)$ $\times 10^{41} = (1.5$ $\pm 0.7)\sigma_{FG}/E_\nu$
Bounds on the angle θ_W in the Weinberg-Salam model	$0.1 \leqslant \sin^2\theta_W$ $\leqslant 0.7$	$\sin^2\theta_W \leqslant 0.45$	...	$0.17 \leqslant \sin^2\theta_W$ $\leqslant 0.33 (\sin\theta_W < 0.65)$ with 90% confidence
Bounds on the angle θ_V in the vector model	$0.2 \leqslant \sin^2\theta_V$ $\leqslant 0.8$	$0.2 \leqslant \sin^2\theta_V$ $\leqslant 0.4$ or $0.6 \leqslant \sin^2\theta_V$ $\leqslant 0.8$	...	$0.2 \leqslant \sin^2\theta_V$ $\leqslant 0.75$

1) The ratio of the NC and CC cross sections for exclusive channels of the same type is of the same order of magnitude as the integrated value R_ν for inclusive cross sections (see Table XI). This means that NC and CC processes are dynamically similar and that there are no particularly distinguished reactions, at least among those that have been studied.

2) The NC single-pion production processes seem to involve the production of the Δ isobar, but with a smaller probability than for CC processes. The weak neutral current therefore contains an isovector component with $\Delta I = 1$.

3) The experimental results are consistent with gauge models, in particular with the Weinberg-Salam model.

4) It remains unclear how large a contribution to the neutral current comes from strange (and charmed?) quarks.

5. NEUTRINO-ELECTRON SCATTERING

A. Experiment

The following data were available by the end of 1975:

1) An experiment using the Gargamelle chamber at CERN, which gave an upper limit on the cross section for the reaction $\nu_\mu + e^- \to \nu_\mu + e^-$.[76]

2) An experiment using the same chamber at CERN, in which three events of the reaction $\bar{\nu}_\mu + e^- \to \bar{\nu}_\mu + e^-$ were detected.[20,76–78]

3) An early experiment using spark chambers at CERN, in which the process $\nu_e + e^- \to \nu_e + e^-$ was not observed.[79,80]

4) An experiment carried out by Reines *et al.*,[81,82] who looked for scattering of electronic antineutrinos from a reactor by electrons: $\bar{\nu}_e + e^- \to \bar{\nu}_e + e^-$; the observed effect was different from zero by a total of two standard deviations.

The results of these experiments are given in Table XIX. We note that $\nu_e e^-$ and $\bar{\nu}_e e^-$ scattering should also occur as a result of the charged currents in the framework of the "old" scheme of Feynman and Gell-Mann.[2] The experiment of Reines *et al.* has not yet reached the accuracy required to make a quantitative test of this scheme. On the other hand, it can be seen from Table XIX that the data of[81,82] lead to more stringent bounds on the Weinberg angle. The range of admissible values of the vector and axial-vector coupling constants is shown by the results[82] in Fig. 15.

B. Theory

According to the V-A weak-interaction scheme, the differential and total cross sections for ν_e scattering with $E_\nu \gg m_e$ can be expressed in terms of the vector and axial-vector coupling constants g_V and g_A as follows:

$$\left.\begin{aligned} \frac{d\sigma}{dE_e} &= \frac{G^2 m_e}{2\pi}\left[(g_V \mp g_A)^2 + (g_V \pm g_A)^2\left(1 - \frac{E_e}{E_\nu}\right)^2\right], \\ \sigma &= \sigma_0 \frac{1}{4}\left[(g_V \mp g_A)^2 + \frac{1}{3}(g_V \pm g_A)^2\right], \\ \sigma_0 &= \frac{2G^2 m_e E_\nu}{\pi} = 1.7 \cdot 10^{-41}\ \text{cm}^2 \cdot E_\nu\ \text{GeV}. \end{aligned}\right\} \quad (65)$$

The upper and lower signs refer to νe^- and $\bar{\nu} e^-$ scattering processes, respectively. In the case of a $V-A$

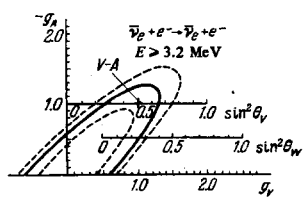

FIG. 15. Restrictions on the coupling constants of the V and A interactions obtained in the experiment of Gurr, Reines, and Sobel.[81]

TABLE XX. Coupling constants of the neutrino-electron interaction.

Model	Constant	$\nu_\mu e$	$\nu_e e$
Weinberg-Salam model	g_V	$-\frac{1}{2}+2\sin^2\theta_W$	$\frac{1}{2}+2\sin^2\theta_W$
	g_A	$\frac{1}{2}$	$-\frac{1}{2}$
Vector model	g_V	$-1+2\sin^2\theta_V$	$2\sin^2\theta_V$
	g_A	0	-1

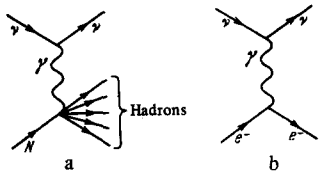

FIG. 17. One-photon exchange diagrams which simulate processes involving neutral currents. a) The νN interaction, b) the νe interaction.

interaction, $\sigma_{\bar{\nu}e}$ is smaller than $\sigma_{\nu e}$ by a factor of three.

In the "old" scheme of Feynman and Gell-Mann, only electronic neutrinos and antineutrinos can be scattered by the electron as a result of the charged currents, and $g_V = -g_A$. Gauge theories contain neutral currents, as a consequence of which muonic neutrinos and antineutrinos can also interact with the electron through the exchange of a neutral meson. The values of the constants g_V and g_A for neutrino-electron scattering in the Weinberg-Salam model were determined by t'Hooft.[83] These values are given in Table XX, together with those calculated according to the vector model.[36]

The cross section (65) is proportional to the electron mass and is therefore small. It rises with energy, so that it is advantageous to perform experiments with large accelerators. Since only a single electron track can be observed in νe scattering, there is a large background due to neutrons and photons.

Figure 16 shows the total cross sections for scattering of the various types of neutrinos by the electron in the Weinberg-Salam model, calculated according to the results in Table XX. We see that none of these cross sections can be arbitrarily small. It is of special interest to note that a sufficiently strong upper limit on $\sigma_{\nu_\mu e}$ imposes bounds on the Weinberg angle θ_W, as well as both upper and lower bounds on the angle θ_V in the vector model. The values of $\sin^2\theta_W$ and $\sin^2\theta_V$ which are allowed by the existing data on νe scattering are shown in Table XIX.

We have so far assumed throughout our discussion

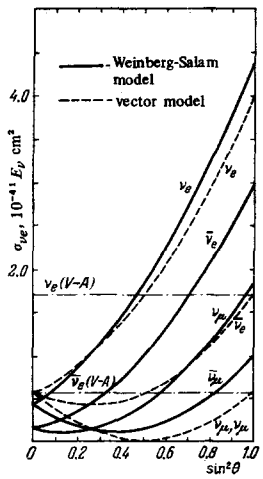

FIG. 16. The cross sections for neutrino-electron and antineutrino-electron scattering in the Weinberg-Salam model (solid curves) and in the vector model (dashed curves) as functions of the angle θ_W or θ_V.

that the weak interaction involving neutral currents is due exclusively to a vector and axial-vector interaction. There are no experimental grounds for this assumption. Although a universal V-A theory is preferable from a theoretical point of view (a massless neutrino of definite helicity can undergo elastic scattering only as a result of a V-A interaction), it would be highly desirable to be able to discriminate between the V-A and the S, P, and T variants experimentally. Unfortunately, this would require difficult experiments to measure the angular and energy distributions and the polarization of the scattered particles. For example, the cross section for elastic scattering of a two-component neutrino by the electron is in general given by the expression[84]

$$\frac{d\sigma}{dy}=\frac{G^2 m_e E_\nu}{2\pi}\Big[(g_V-g_A)^2+(g_V+g_A)^2y^2+\frac{1}{2}(g_S^2+g_P^2)(1-y)^2 + g_T^2(1+y)^2-g_T(g_S+g_P)(1-y^2)+\frac{m_e}{E_\nu}(1-y)(g_A^2-g_V^2+g_S^2-g_T^2)\Big], \tag{66}$$

where

$$y=\frac{E'_\nu}{E_\nu}=1-\frac{E_e}{E_\nu}, \tag{67}$$

and the weak-interaction coupling constants are normalized to $G/\sqrt{2}$ and are real by virtue of the assumption of CP invariance. It is easy to see that an S, P, or T interaction in general contains a term linear in y, even for $m_e \ll E_\nu$, so that it is in principle different from the V-A interaction. On the other hand, by choosing the constants g_S, g_P, and $g_T=\sqrt{g_S^2+g_P^2}$, it is possible to reproduce the spectrum which is characteristic of g_V and g_A; provided that $|g_V|\neq|g_A|$, the last term in (66), which is important only at very low neutrino energies, is different for the V-A and the S, P, and T interactions. When the neutrino energy is large in comparison with the electron mass, it is possible to distinguish between the two variants of the weak interaction only by means of polarization experiments.

C. Weak interaction or electric radius?

Although neutrinos are neutral particles and have no static charges, they may in principal have a non-zero electric radius or an anomalous magnetic moment (the latter is possible only if the neutrino mass is non-zero). In this case, the diagrams shown in Fig. 17 simulate a weak interaction involving neutral currents. If there is an electric radius, the factors q^2 in the vertex and $1/q^2$ in the propagator cancel; the effective interaction is therefore a contact interaction similar to the ordinary weak interaction. The interaction with a magnetic moment is more specific. Both variants have been dis-

TABLE XXI. Values of the electric radius of the neutrino required to explain the experimental data by means of an electromagnetic interaction.

Process	Laboratory	Energy range, GeV	Values of $\lvert r_\nu^2\rvert$, 10^{-31} cm²	
			Neutrino reaction	Antineutrino reaction
$\nu_\mu(\bar\nu_\mu)+N\to\nu_\mu(\bar\nu_\mu)+\dots$	CERN	1—40	4.0±0.4	3.8±0.4
	HPW	5—200	2.9±0.3	3.0±0.5
	Caltech-Fermilab (1974)	20—150	4.2	3.0
$\nu_\mu(\bar\nu_\mu)+e^-\to\nu_\mu(\bar\nu_\mu)+e^-$ (90% confidence)	CERN	1—10	<2.5	<2.1
$\bar\nu_e+e^-\to\bar\nu_e+e^-$	Irvine (Savannah River reactor)	0—0.01	—	<2.5

cussed by a number of authors, in particular in[85-87].

We shall now show that when the data on the inclusive cross sections for ν-nucleon interactions involving neutral currents are compared with the data on neutrino-electron scattering, it becomes doubtful that an "electromagnetic" explanation of these two processes is possible (the calculations which follow have been made in collaboration with A. N. Ivanov).

The only unknown quantity in the diagrams of Fig. 17 is the value of the electric radius or the magnetic moment of the neutrino; the lower part of Fig. 17a is the same as that of the electron-nucleon interaction, and its square is given by the known structure functions W_1 and W_2. If we assume that there is no weak interaction involving NCs and that the experimentally observed effects are due entirely to the electromagnetic radius, i.e., to a neutrino interaction of the form

$$e\frac{r_\nu^2 q^2}{6}(\bar\nu\gamma_\alpha\nu), \tag{68}$$

then the inclusive cross sections for neutrino-nucleon interactions are given by

$$\begin{aligned}\frac{1}{2}[\sigma(\nu_\mu+p\to\nu_\mu+\dots)+\sigma(\nu_\mu+n\to\nu_\mu+\dots)]\\ =\frac{1}{2}[\sigma(\bar\nu_\mu+p\to\bar\nu_\mu+\dots)+\sigma(\bar\nu_\mu+n\to\bar\nu_\mu+\dots)]\\ =\frac{2\pi}{27}C\alpha^2 r_\nu^4 ME_\nu=(3.7\pm0.5)\,10^{-6}r_\nu^4 ME_\nu,\end{aligned} \tag{69}$$

where M is the nucleon mass, $\alpha=e^2/4\pi$, and

$$C=\int_0^1[f^{ep}(x)+f^{en}(x)]\cdot 2x\,dx=0.30\pm0.04. \tag{70}$$

The derivation of this result assumes the importance of the region of large q^2, where scaling is valid, i.e., where ($\nu=q_0$ is the energy of the virtual photon)

$$MW_1=f(x),\quad \nu W_2=2xf(x),\quad x=-\frac{q^2}{2M\nu}. \tag{71}$$

As regards scattering of the muonic neutrino by the electron, this process is determined by the relations (65), where for $\nu_\mu e$ and $\bar\nu_\mu e$ scattering we have

$$g_A=0,\quad g_V=\frac{\pi\alpha\sqrt{2}}{3G}r_\nu^2, \tag{72}$$

while for $\nu_e e$ and $\bar\nu_e e$ scattering we have

$$g_A=-1,\quad g_V=1+\frac{\pi\alpha\sqrt{2}}{2G}r_\nu^2, \tag{73}$$

and r_ν^2 can in general be either positive or negative.

The experimental data contained in Tables X, XI, and XX and in Fig. 15 lead to the values of r_ν^2 given in Table XXI. It can be seen that the inclusive experiments using nucleon targets are in mutual agreement and yield the value

$$|r_\nu^2|=(3.4\pm0.5)\cdot10^{-31}\ \text{cm}^2, \tag{74}$$

which, however, exceeds the results of a number of theoretical calculations[88-95] by more than an order of magnitude. Such a large value of the neutrino radius can be obtained only by adopting very strong additional hypotheses, such as that of the "zero-charge" pole in the Green's function.[96] On the other hand, experiments on scattering of muonic neutrinos by the electron give an upper limit on $|r_\nu^2|$ which is only half as large at the 90% confidence level. Therefore it seems doubtful that the experimental data on NCs can be described in terms of an electromagnetic interaction involving an electric radius of the neutrino.

The possibility of describing the experimental data by assuming that the neutrino has an anomalous magnetic moment can be ruled out. Although the results of individual inclusive experiments do not contradict the assumption that the neutrino has an electromagnetic interaction of the form $(e\varkappa/2m_e)(\bar\nu\sigma_{\alpha\beta}q_\beta\nu)$ with $\varkappa=(1.5\pm0.2)\times10^{-6}$, the cross section for neutrino scattering in this case would have an energy dependence $\sigma\sim\ln^2 s$, in contrast with the dependence $\sigma\sim s$ for a contact four-fermion interaction. Since $s=2m_{\text{targ}}\times E_\nu$, the ordinary interaction requires νe cross sections which are three orders of magnitude smaller than the νN interaction. With the dependence $\sim\ln^2 s$, there is no such suppression. The experimental data unambiguously favor the first possibility: in the energy region $E_\nu\sim1$ GeV, we have $\sigma(\nu_\mu e)\sim10^{-42}$ cm², while $\sigma(\nu_\mu N)\sim\sigma(\bar\nu_\mu N)\sim10^{-39}$ cm².

D. What can we learn from neutrino-electron scattering experiments?

1) The fact that the process $\bar\nu_\mu+e^-\to\bar\nu_\mu+e^-$ is observed indicates that the neutral current involves not only hadrons (or quarks) and neutrinos, but also electrons. In other words, the NC interaction is universal, although the nature of this universality is not yet completely clear.

2) It is not possible to achieve a consistent description of the data on scattering of muonic neutrinos and antineutrinos by nucleons and electrons in terms of a purely electromagnetic interaction. This shows that a weak interaction involving neutral currents actually exists.

3) The experimental results are in agreement with the Weinberg-Salam model or the vector model, and rather stringent bounds are found on the angles θ_W or θ_V.

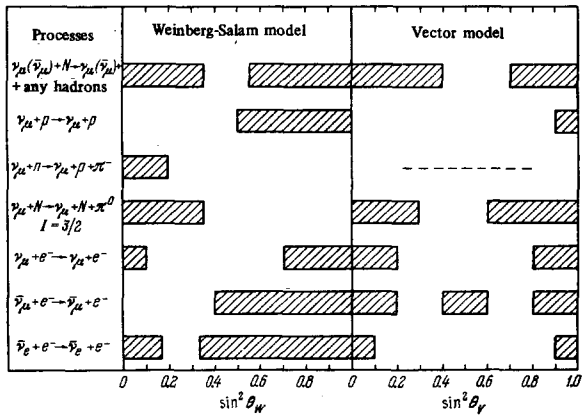

FIG. 18. Values of the angles θ_W and θ_V allowed by the various experiments. The cross-hatched bands show the forbidden values of $\sin^2\theta_W$ and $\sin^2\theta_V$.

6. CONCLUSIONS

The weak interaction due to neutral currents is being studied very widely. The results obtained so far are in essence preliminary and may still change. Nevertheless, we can already conclude that the interaction of muonic neutrinos with nucleons or electrons involves processes which are not accompanied by muon emission and which are therefore governed by the weak interaction due to neutral currents. The strength of this interaction is comparable with that of the ordinary weak interaction due to charged currents, differing from the latter by a coefficient 1/4 in the case of neutrino scattering or 1/2 in the case of the antineutrino interaction.

Perhaps the most interesting experimental fact is the equality of the NC inclusive cross sections for neutrinos and antineutrinos. It remains unclear whether this equality is due to the presence of only a single V (or A) variant in the neutral current, i.e., to the conservation of parity, or whether it is accidental and holds only for a target consisting of approximately equal numbers of protons and neutrons.

The existing data are consistent with gauge models of the weak interaction, in particular with the Weinberg-Salam model with

$$\sin^2\theta_W \sim \frac{1}{3} \tag{75}$$

or the vector model with

$$\sin^2\theta_V \sim \frac{2}{3}. \tag{76}$$

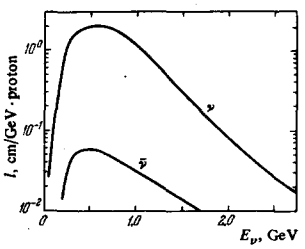

FIG. 19. The neutrino spectrum and antineutrino background at Argonne.[52]

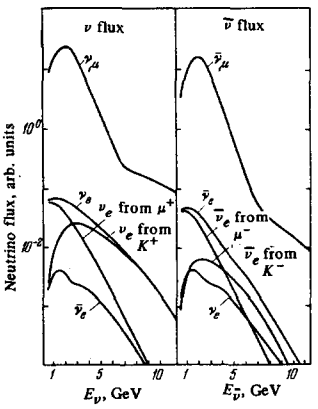

FIG. 20. The calculated neutrino and antineutrino spectra at CERN.[97]

A summary of the bounds on these angles which follow from the various experiments is given in Fig. 18.

Finally, we list several experiments which might shed light on the remaining open questions.

a) The inclusive neutrino-nucleon interaction has generally been studied until now using light nuclei containing approximately equal numbers of protons and neutrons. It would also be desirable to obtain data using heavy nuclei or hydrogen-rich compounds such as propane, in order to ascertain whether the ratio of neutrino and antineutrino NC cross sections depends on the composition of the target.

b) Current investigations of the dependence of inclusive cross sections on the total energy of the hadrons will in principle provide a means of obtaining restrictions on the allowed variants of the weak interaction and testing the predictions of very specific gauge models for this interaction.

c) Of the various inclusion experiments, it would be of special interest to observe the elastic scattering of neutrinos and antineutrinos by the proton. Such experiments would make it possible in principle to obtain information on the values of the coupling constants and form factors of the weak interaction involving NCs.

d) It would be highly desirable to obtain more accurate data on reactions involving single pion production. To begin with, it is necessary to eliminate the inconsistencies between the data of the various groups shown in Table XVI. What is of interest here from the theoretical point of view is the ratio of the cross sections for production of the $N+\pi$ system in the states with isospin 3/2 and 1/2.

e) It would also be of interest to study the reaction

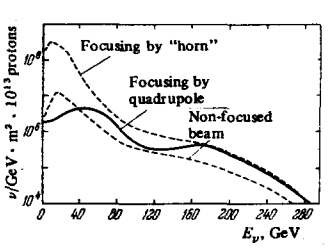

FIG. 21. The calculated neutrino and antineutrino spectra at Serpukhov.[98]

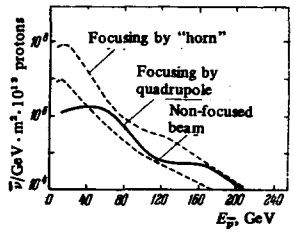

FIG. 22. The neutrino and antineutrino spectra at Batavia (HPW group).[99]

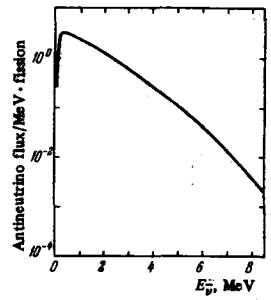

FIG. 24. The calculated spectrum of electronic antineutrinos from the β decay of the fission products of U^{235}.[101]

$\nu_\mu + N \to \nu_\mu + \Lambda + K$, in which the $\Lambda + K$ system is in an isotopically pure state with $I = 1/2$. As we have already pointed out, an analysis of this reaction at small momentum transfers would make it possible to estimate the contribution from strange quarks to the neutral current.

f) Although difficult to carry out, elastic neutrino-electron or antineutrino-electron scattering remains the "cleanest" type of experiment to determine the coupling constants of the weak interaction involving the neutral current.

Hopefully, answers to the foregoing questions will be obtained in the near future.

APPENDIX: NEUTRINO SPECTRA

Neutrino experiments are performed using very cumbersome equipment, which takes a long time to prepare. It appears that all such experiments in the near future will be carried out using neutrino beams that are already in existence; there are no plans at the present time to obtain new beams. In this connection, it seems expedient to summarize the data on the neutrino spectra which are available at various laboratories. These spectra are shown in Figs. 19–24. Some brief remarks follow.

1. The number of neutrinos is generally much greater than the number of antineutrinos, since pp collisions lead to the production of many more π^+ and K^+ mesons than π^- and K^- mesons.

2. The spectrum of neutrinos at Brookhaven has not been published, but it must obviously be similar to the spectrum at CERN.

3. Figure 20 shows the admixture of electronic neutrinos (antineutrinos) in the beam of muonic neutrinos (antineutrinos), and Fig. 23 shows the admixture of antineutrinos $\bar{\nu}_\mu$ in the beam of neutrinos ν_μ and vice versa.

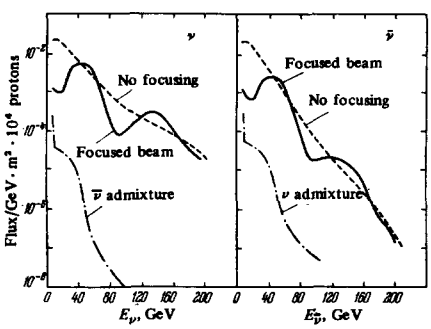

FIG. 23. The calculated neutrino and antineutrino spectra at Batavia (narrow beams of the Caltech-Fermilab group).[100]

4. The spectra shown in Fig. 22 correspond to three different experimental conditions: a non-focused neutrino beam (which has the advantage of minimal errors in the determination of the flux), a beam obtained using a focusing magnet (horn), and a beam obtained using a quadrupole magnet.

5. Figure 23 shows the results for a non-focused beam and a "narrow" beam obtained by selecting pions and kaons with a definite momentum.

Note added in proof (June 1976). Some new results have recently been obtained by the HPW group:

1. Data on the ratio $(\sigma_{\bar{\nu}}/\sigma_\nu)_{NC}$ for $E_\nu = 40$–80 GeV were presented at the conference on neutrino physics at Aachen (June 1976).[102] The value of this ratio depends on a continuation into the region of small hadron energies and hence on an assumption about the variant of the weak interaction involving NCs. In the case of the vector interaction, the result differs from unity by three standard deviations (0.40 ± 0.17). This is regarded as an argument against the vector model.[36–38]

2. The HPW experiment carried out at Brookhaven[103] and the experiment of the Columbia-Illinois-Rockefeller group[104] gave the following results for elastic neutrino-proton scattering:

$$\frac{\sigma(\nu_\mu p \to \nu_\mu p)}{\sigma(\nu_\mu n \to \mu^- p)} = \begin{cases} 0.17 \pm 0.05 \text{ (HPW)}, \\ 0.23 \pm 0.09 \text{ (CIR)}. \end{cases}$$

The form of the differential cross section as a function of momentum transfer is at variance with the prediction of the vector model but is consistent with that of the Weinberg-Salam model.[105]

3. The HPW group has also reported that the ratio of the CC cross sections, $(\sigma_{\bar{\nu}}/\sigma_\nu)_{CC}$, becomes energy-dependent with increasing neutrino energies, with a variation from ~ 0.4 (20 GeV) to ~ 0.7 (80 GeV).[106] This result is at variance with the data shown in Figs. 10 and 11, and (if confirmed) it tends to indicate that new heavy particles are produced in the antineutrino-nucleon interaction.

CITED LITERATURE[2)]

[1]V. A. Alekseev, B. Ya. Zel'dovich, and I. I. Sobel'man, Usp. Fiz. Nauk **118**, 385 (1976). A. N. Moskalev, R. M. Ryndin, and I. B. Khriplovich, *ibid.*, p. 409.
[2]R. P. Feynman and M. Gell-Mann, Phys. Rev. **109**, 193 (1958).
[3]E. C. G. Sudarshan and R. E. Marshak, *ibid.*, p. 1860.
[4]N. Cabibbo, Phys. Rev. Lett. **10**, 531 (1963).
[5]M. Roos, Phys. Lett. **B36**, 130 (1971); private communication (cited by K. Kleinheit, in: London, III-23).
[6]Particle Data Group, Review of Particle Properties, Phys. Lett. **B50**, 1 (1974).
[7]S. Bludman, Nuovo Cimento **9**, 433 (1958).
[8]Ya. B. Zel'dovich, Zh. Eksp. Teor. Fiz. **36**, 964 (1959) [Sov. Phys. JETP **9**, 682 (1959)].
[9]S. B. Treiman, Nuovo Cimento **15**, 916 (1959).
[10]V. N. Baĭer and I. B. Khriplovich, Zh. Eksp. Teor. Fiz. **39**, 1374 (1960) [Sov. Phys. JETP **12**, 959 (1961)].
[11]B. M. Pontecorvo, Zh. Eksp. Teor. Fiz. **43**, 1521 (1962) [Sov. Phys. JETP **16**, 1073 (1963)].
[12]S. S. Gershteĭn, Nguyen Van Hieu, and R. A. Éramzhyan, *ibid.*, p. 1554 [p. 1097].
[13]G. t'Hooft, Nucl. Phys. **B35**, 167 (1971).
[14]S. Weinberg, Phys. Rev. Lett. **19**, 1264 (1967).
[15]A. Salam, in: Elementary Particle Theory, Ed. N. Svartholm, Stockholm, Almquist an Forlag A. B., 1968, p. 367.
[16]A. I. Vaĭnshteĭn and I. B. Khriplovich, Usp. Fiz. Nauk **112**, 685 (1974) [Sov. Phys. Usp. **17**, 263 (1974)].
[17]F. J. Hasert *et al.*, Phys. Lett. **B46**, 138 (1973); Nucl. Phys. **B73**, 1 (1974).
[18]A. Pullia, in: London, IV-114.
[19]W. E. Fry and D. Haidt, Report CERN 75-1.
[20]CERN-Gargamelle Collaboration, presented by J. Morfin to the Stanford Electron-Photon Conference (1975), cited by F. J. Sciulli, Caltech preprint CALT 68-520, 1975.
[21]A. Benvenuti *et al.*, Phys. Rev. Lett. **32**, 800 (1974).
[22]B. Aubert *et al.*, *ibid.*, p. 1454.
[23]C. Ribbia, in: London, IV-117.
[24]A. K. Mann, in: Paris, p. 273.
[25]B. C. Barish *et al.*, Phys. Rev. Lett. **34**, 538 (1975).
[26]B. C. Barish, in: Paris, p. 291.
[27]D. C. Cundy, in: London, IV-131.
[28]T. Eichten *et al.*, Phys. Lett. **B46**, 274, 281 (1973).
[29]M. Hagunauer, in: London, IV-95.
[30]A. Benvenuti *et al.*, Phys. Rev. Lett. **32**, 1250 (1974).
[31]R. Imlay, in: London, IV-100.
[32]F. Sciulli, *ibid.*, IV-105.
[33]B. C. Barish *et al.*, Phys. Rev. Lett. **35**, 1316 (1975).
[34]R. P. Feynman, Photon-Hadron Interactions, Benjamin, 1972 (Russ. Transl., Mir, Moscow, 1975).
[35]D. H. Perkins, Review Talk at the International Symposium on Lepton and Photon Interactions at High Energies, Stanford, 1975.
[36]A. De Rujula, H. Georgi, and S. L. Glashow, Phys. Rev. **D12**, 3589 (1975).
[37]R. M. Barnett, Phys. Rev. Lett. **34**, 1 (1975). H. Harari, Phys. Lett. **B57**, 265 (1975). F. A. Wilczek, A. Zee, R. L. Kingsley, and S. B. Treiman, Phys. Rev. **D12**, 2768 (1975).
[38]H. Fritzsch and P. Minkowski, Caltech preprint CALT 68-503 (1975). H. Fritzsch, M. Gell-Mann, and P. Minkowski, Phys. Lett. **B59**, 256 (1975).
[39]L. M. Sehgal, Nucl. Phys. **B65**, 141 (1973).
[40]C. N. Albright, *ibid.* **B70**, 486 (1974).
[41]A. Pais and S. B. Treiman, Phys. Rev. **D6**, 2700 (1972).
[42]E. A. Paschos and L. Wolfenstein, *ibid.* **D7**, 91 (1973).
[43]D. C. Cundy *et al.*, Phys. Lett. **B31**, 479 (1970).
[44]E. Escoubes, in: Paris, p. 265.
[45]P. Schreiner, in: London, IV-123.
[46]T. D. Lee and C. N. Yang, Phys. Rev. Lett. **4**, 307 (1960).
[47]N. Cabibbo and R. Gatto, Nuovo Cimento **15**, 304 (1960).
[48]Y. Yamaguchi, Progr. Theor. Phys. **23**, 1117 (1960).
[49]S. Weinberg, Phys. Rev. **D5**, 1412 (1972).
[50]V. I. Zakharov, in: Élementarnye chastitsy (Elementary Particles), No. 2, Atomizdat, Moscow, 1975, p. 59.
[51]S. J. Barish *et al.*, Phys. Rev. Lett. **33**, 448 (1974).
[52]L. G. Hyman, in: Paris, p. 183.
[53]I. Budagov *et al.*, Phys. Lett. **B29**, 524 (1969),
[54]D. H. Perkins, in: Proc. of the 16th Intern. Conf. on High Energy Physics, Vol. 4, Batavia, 1972, p. 189.
[55]A. Rousset, in: London, IV-128.
[56]J. P. Vialle, in: Paris, p. 225.
[57]F. J. Hasert *et al.*, Phys. Lett. **B59**, 485 (1975).
[58]E. G. Gazzoli, in: Paris, p. 239.
[59]W. Y. Lee, Phys. Lett. **B40**, 423 (1972).
[60]W. Y. Lee, in: London, IV-127. W. Y. Lee, in: Paris, p. 205.
[61]H. Faissner, in: Balaton, Vol. 1, p. 116. H. Baldo-Ceolin, *ibid.*, p. 166.
[62]C. H. Albright *et al.*, Phys. Rev. **D7**, 2220 (1973).
[63]S. L. Adler, *ibid.* **D9**, 229 (1974).
[64]S. L. Adler, S. Nussinov, and E. A. Paschos, *ibid.*, p. 2125.
[65]A. F. Garfinkel, in: Paris, p. 311.
[66]S. J. Barish *et al.*, Phys. Rev. Lett. **36**, 179 (1976).
[67]S. Galster *et al.*, Phys. Rev. **D5**, 519 (1972).
[68]J. Campbell *et al.*, Phys. Rev. Lett. **30**, 335 (1973).
[69]S. J. Barish *et al.*, *ibid.* **33**, 1446 (1974).
[70]U. Nguen Khac, in: Paris, p. 173.
[71]H. Deden *et al.*, Phys. Lett. **B58**, 361 (1975).
[72]S. L. Glashow, J. Illiopulos, and L. Maiani, Phys. Rev. **D2**, 1285 (1970).
[73]H. S. Gurr, F. Reines, and H. W. Sobel, Phys. Rev. Lett. **33**, 179 (1974).
[74]Yu. V. Gaponov and I. V. Tyutin, Zh. Eksp. Teor. Fiz. **47**, 1826 (1964). [Sov. Phys. JETP **20**, 1231 (1965)].
[75]T. W. Donnely *et al.*, Phys. Lett. **B49**, 8 (1974).
[76]F. J. Hasert *et al.*, *ibid.* **B46**, 121 (1973).
[77]J. Sacton, in: London, IV-121.
[78]F. J. Hasert, in: Paris, p. 257.
[79]J. K. Bienlein *et al.*, Phys. Lett. **13**, 80 (1964).
[80]H. J. Steiner, Phys. Rev. Lett. **24**, 746 (1970).
[81]H. S. Gurr, F. Reines, and H. W. Sobel, *ibid.* **28**, 1406 (1972).
[82]F. Reines, H. W. Sobel, and H. S. Gurr, in: Balaton, Vol. 1, p. 74.
[83]G. t'Hooft, Phys. Lett. **B37**, 195 (1971).
[84]V. M. Shekhter, Zh. Eksp. Teor. Fiz. **34**, 257 (1958) [Sov. Phys. JETP **7**, 179 (1958)].
[85]V. I. Andryushin, S. M. Bilen'kiĭ, and S. S. Gershteĭn, Pis'ma Zh. Eksp. Teor. Fiz. **13**, 573 (1971) [JETP Lett. **13**, 409 (1971)].
[86]D. Yu. Bardin and O. A. Mogilevsky, Lett. Nuovo Cimento **9**, 549 (1974).
[87]J. E. Kim, V. S. Mathur, and S. Okubo, Phys. Rev. **D9**, 3050 (1974).
[88]Ya. B. Zel'dovich and A. M. Perelomov, Zh. Eksp. Teor. Fiz. **39**, 1115 (1960) [Sov. Phys. JETP **12**, 777 (1961)].
[89]J. Bernstein and T. D. Lee, Phys. Rev. Lett. **11**, 512 (1963).
[90]W. K. Cheng and S. A. Bludman, Phys. Rev. **136**, B1787 (1964).
[91]T. D. Lee and A. Sirlin, Rev. Mod. Phys. **36**, 666 (1964).
[92]Ph. Meyer and D. Schiff, Phys. Lett. **8**, 217 (1964).

[2)]We employ the following abbreviations: London—Proceedings of the 17th International Conference on High Energy Physics (London, 1974); Paris—La Physique du Neutrino à Haute Energie, Ecole Polytechnique (Paris, 1975); Balaton—Neutrino-75, Proceedings of the IUPAP Conference, Balatonfüred, Hungary, 1975.

[93]R. N. Choudhuri and R. Dutt, Phys. Rev. D1, 2945 (1970).
[94]P. Castoldi, Lett. Nuovo Cimento 3, 281 (1972),
[95]L. F. Landovitz and W. Schreiner, Phys. Rev. D7, 3014 (1973).
[96]B. A. Arbuzov, IHEP preprint STR 74-98, 1974.
[97]P. Musset, CERN report TC-L/Int. 74-9, 1974.
[98]E. V. Eremenko *et al.*, in: Paris, p. 331.
[99]A. Benvenuti *et al.*, *ibid.*, p. 397.
[100]P. Limon *et al.*, Nucl. Instr. and Meth. 116, 317 (1974).
[101]F. T. Avignone, Phys. Rev. D2, 2609 (1970).
[102]A. Benvenuti *et al.*, Preprint HPWF-76/4, 1976.
[103]D. Cline *et al.*, Preprint PRE 19906, 1976.
[104]W. Y. Lee *et al.*, Columbia preprint, 1976.
[105]C. H. Albright *et al.*, Preprint FERMILAB-Pub-76/45-THY, 1976.
[106]A. Benvenuti *et al.*, Preprint HPWF-76/2, 1976.

Translated by N. M. Queen

Installations for the investigation of free neutrinos

B. M. Pontecorvo

Joint Institue for Nuclear Research, Dubna
Usp. Fiz. Nauk **119**, 633–639 (August 1976)

PACS numbers: 29.90.+r, 92.80.+r

Neutrino physics and its applications to astrophysics constitute an independent branch of a blossoming science. In the course of preparing a review lecture on neutrino physics and astrophysics, I searched for a compact exposition form capable of giving the listeners an idea of the scales and the progress of the branch of physics in question. For this purpose I prepared several tables of existing installations for free-neutrino research. The tables, in the opinion of the editors of this journal, can be of interest to its readers and are presented below.

The table includes most installations for which means have been allocated, i.e., installations either already in operation or actually under construction (an exception is the DUMAND installation, the actual construction of which is still in doubt, but is reported here because of its exotic character).

Four tables are presented in accordance with the following arbitrary subdivision:

I. Installations for manmade neutrinos of "low" energies.

II. Installations for the investigation of manmade neutrinos of high energies.

III. Installations for the investigation of "low"-energy cosmic neutrinos.

IV. Installations for the investigation of high-energy cosmic neutrinos.

The information contained in the tables is frequently tentative for objective reasons, for subjective reasons (insufficient information available to the author of the tables), and for reasons connected with limiting volume of the tables themselves. The bibliography, of course, is far from complete and is chosen mainly to include the latest data on the given group.

TABLE I. Installations for the investigation of "low" energy manmade neutrinos.

Research group or laboratory	Neutrino energy	Source of neutrinos	Flux of neutrinos near detector; number of events	Distance between detector and source, m	Investigations	Type of detector
Los Alamos[1]	Several MeV ($\tilde{\nu}_e$)	Fission products in "Savannah River" reactor	$\sim 10^{13}$ cm^{-2} sec^{-1}	~ 13 m	Observation of free neutrinos in inverse β-decay reactions	Scintillation counters
University of California[2]	Several MeV ($\tilde{\nu}_e$)	Fission products in "Savannah River" reactor	$\sim 2 \cdot 10^{13}$ cm^{-2} sec^{-1}; ≤ 1 events/day	~ 13 m	Search for the processes $\tilde{\nu}_e + e \to \tilde{\nu}_e + e$	Scintillation counters
LAMPF (projected, but many parts already completed)[3]	10–50 MeV (ν_e, ν_μ, $\tilde{\nu}_\mu$)	Stopped pions and muons in meson factories	~ 1 event of $\nu_e - e$ scattering per day	~ 7	$\nu_e - e$ scattering; $\nu_\mu - e$ scattering; conservation of lepton charge, etc.	Electronic and radiochemical methods
Nuclear Physics Institute, USSR Academy of Sciences (projected)[4]	10–300 MeV (ν_e, $\tilde{\nu}_e$, ν_μ, $\tilde{\nu}_\mu$)	Muons accumulated in a superconducting trap and decaying in flight	~ 10 events of $\nu_e - e$ scattering per day with accelerator of the LAMPF type	~ 7	$\mu_e - e$ scattering; neutral currents (excitation of nuclei)	Electronic registration methods; detector weighing several tons